# *Late Miocene erosion and evolution of topography along the western slope of the Colorado Rockies*





| | |
|---|---|
| **Citation** | Rosenberg, R., Kirby, E., Aslan, A., Karlstrom, K., Heizler, M., & Ouimet, W. (2014). Late Miocene erosion and evolution of topography along the western slope of the Colorado Rockies. Geosphere, 10(4), 641-663. doi:10.1130/GES00989.1 |
| **DOI** | 10.1130/GES00989.1 |
| **Publisher** | Geological Society of America |
| **Version** | Accepted Manuscript |
| **Terms of Use** | http://cdss.library.oregonstate.edu/sa-termsofuse |

# Late Miocene erosion and evolution of topography along the western slope of the Colorado Rockies

**Russell Rosenberg[1], Eric Kirby[2], Andres Aslan[3], Karl Karlstrom[4], Matt Heizler[5], Will Ouimet[6]**

[1] *Penn State University, Department of Geosciences, University Park, Pennsylvania 16802, USA*
[2] *Oregon State University, College of Earth, Ocean, and Atmospheric Sciences, Corvallis, Oregon 97330, USA*
[3] *Colorado Mesa University, Department of Physical and Environmental Sciences, Grand Junction, Colorado 81501, USA*
[4] *University of New Mexico, Department of Earth and Planetary Sciences, Albuquerque, New Mexico 87131, USA*
[5] *New Mexico Bureau of Geology and Mineral Resources, New Mexico Tech, Socorro, New Mexico 878011, USA*
[6] *University of Connecticut, Department of Geography, Storrs, Connecticut 06269, USA*

**ABSTRACT**

In the Colorado Rocky Mountains, the association of high topography and low seismic velocity in the underlying mantle suggests that recent changes in lithospheric buoyancy may have been associated with surface uplift of the range. This paper examines the relationships among late Cenozoic fluvial incision, channel steepness, and mantle velocity domains along the western slope of the northern Colorado Rockies. New $^{40}Ar/^{39}Ar$ ages on basalts capping the Tertiary Browns Park Formation range from ~11-6 Ma and provide markers from which we reconstruct incision along the White, Yampa and Little Snake Rivers. The magnitude of post-10 Ma incision varies systematically from north to south, increasing from ~500 m along the Little Snake River to ~1500 m along the Colorado River. Spatial variations in the amount of late Cenozoic incision are matched by metrics of channel steepness; the upper Colorado River and its tributaries (e.g. Gunnison and Dolores Rivers) are two to three times greater than the Yampa and White Rivers, and these variations are independent of both discharge and lithologic substrate. The coincidence of steep river profiles with deep incision suggests that the fluvial systems are dynamically adjusting to an external forcing, but is not readily explained by a putative increase in erosivity

associated with late Cenozoic climate change. Rather, channel steepness correlates with the position of the channels relative to low velocity mantle. We suggest that the history of late Miocene – present incision and channel adjustment reflects long-wavelength tilting across the western slope of the Rocky Mountains.

## INTRODUCTION

One of the outstanding tectonic questions in western North America regards the development and support of high topography (Figure 1). It has long been recognized that correlations exist among high topography (Gregory and Chase, 1994), low seismic velocity mantle (Grand, 1994; Schmandt and Humphreys, 2010), high heat flow (Sass et al., 1971; Reiter, 2008), relatively thin crust (Sheehan et al., 1995; Hansen et al., 2013), and extrusive volcanism (Larson et al., 1975; Kunk et al., 2002). Although these data point to a role for mantle buoyancy in support of high topography, questions remain about when and how such buoyancy was established. A variety of potential mechanisms have been proposed, including: hydration of lithospheric mantle (Humphreys et al., 2003) and/or thermal re-equilibration following removal of the Laramide slab (Roy et al., 2004; Roy et al., 2009), delamination and/or removal of lithospheric mantle (Elkins-Tanton, 2005; Levander et al., 2011), and changes in the mantle flow field due to small-scale convection (Moucha et al., 2008; van Wijk et al., 2010; Liu and Gurnis, 2010; Forte et al., 2010).

Recent geophysical studies focused on the Colorado Rockies (Aster et al., 2009; Schmandt and Humphreys, 2010) reveal a prominent region of anomalously slow P- and S-wave speeds (Coblentz et al., 2011; Karlstrom et al., 2012) that resides in the upper mantle beneath the region of highest topography (Fig. 2). This observation reaffirms previous conclusions that support of high topography in Colorado largely resides in the upper mantle (Sanheehan et al., 1995; Grand, 1994). In fact, the Colorado Rockies exhibit some of the thinnest crust along the range, and a negative correlation between crustal thickness and high topography also favors mantle support for high topography (Hansen et al., 2013). The timing of when this buoyancy was established, however, is not known directly.

The timing and patterns of incision along fluvial systems within and adjacent to the Rocky Mountains suggests a possible role for differential uplift of the range relative to the Colorado Plateau and Great Plains. In the northern Colorado Rockies, the onset of fluvial incision appears to coincide with the cessation of late Tertiary deposition in intermontane basins (Larson et al., 1975; Buffler, 2003; McMillan et al., 2006). Along the eastern flank of the range, incision post-dates deposition of the ca. 18 - 6 Ma Ogallala Formation (McMillan et al., 2002; McMillan et al., 2006). Notably, reconstruction of paleo-transport gradients (McMillan et al., 2002; Duller et al., 2012) in these deposits argues for long-wavelength tilting in excess of that expected for a simple isostatic response to exhumation (e.g., Leonard, 2002). Thus, some conclude that tilting must have been, in part, driven by surface uplift within the Rockies (McMillan et al., 2002; Riihimaki et al., 2007; Duller et al., 2012; Nereson et al., 2013), but others argue that most, if not all, recent incision may reflect climatically modulated changes in erosive efficiency (e.g., Anderson et al., 2006; Wobus et al., 2010).

Along the western slope of the range, fluvial incision also appears to have initiated in the past ~10 Ma (Kunk et al., 2002; Berlin, 2009; Aslan et al., 2008; Aslan et al., 2010; Karlstrom et al., 2012), but the mechanisms driving incision remain uncertain. In particular, the possibility that incision along the western slope reflects upstream migration of a wave of transient incision in response to drainage integration along the Colorado and Green Rivers (e.g., Pederson et al., 2002, 2013) presents an additional complication. In an effort to determine whether late Tertiary incision along the western slope reflects differential rock uplift associated with changes in mantle buoyancy (Aslan et al., 2010; Karlstrom et al., 2012; Darling et al., 2012), we examine the White, Yampa, and Little Snake Rivers in Colorado (Figure 2). Recent analyses of the regional patterns of channel steepness ($k_{sn}$, a measure of channel slope normalized for contributing drainage area, Kirby and Whipple, 2012) reveal spatial differences that appear to correspond to the position of rivers relative to low-velocity mantle beneath the range (Karlstrom et al., 2012) and do not reflect spatial differences in discharge (Pederson and Tressler, 2012). In this paper we present a detailed analysis of river longitudinal profiles and their relationship to substrate lithology and combine this analysis with new $^{40}Ar/^{39}Ar$ ages of late Cenozoic basalts that provide new constraints on the timing and magnitude of fluvial incision. Collectively, these observations reveal spatial patterns in both channel steepness and in the magnitude of post-10 Ma incision that help deconvolve the relative roles of climate change, drainage integration, and/or differential rock uplift along the western flank of the Rockies.

## TIMING AND MAGNITUDE OF INCISION ALONG THE WESTERN SLOPE OF THE COLORADO ROCKIES

### Background: Previous Work on Late Cenozoic Incision

#### *Colorado River System*

Much of the evidence for late Cenozoic tectonism in the Rocky Mountains relies on the history of incision along major drainages (e.g., McMillan et al., 2006; Riihimaki et al., 2007). An extensive body of work over the past two decades indicates that the Colorado River has incised ~1100-1500 m across the western slope of the Rockies during the past 10 Ma (e.g., Larson et al., 1975; Kunk et al., 2002; Aslan et al., 2010). We briefly summarize these constraints below; relevant data are compiled in Table 1 and shown for reference on Figure 3. Following Kunk et al. (2002), we exclude sites from within regions known to have experienced collapse during evaporite dissolution.

Most of the key markers used to reconstruct fluvial incision along the main stem of the Colorado River rely on associations of fluvial gravels representing ancestral river deposits with basalt flows (Table 1). The westernmost of these is located at Grand Mesa, just upstream from Grand Junction, CO (Figure 3), where the basal basalt flow (10.8 +/- 0.2 Ma; Kunk et al., 2002) overlies river gravels at ~1500 m above the present-day river (Aslan et al., 2010). Farther upstream, the Colorado River flows between Battlement Mesa and Mt. Callahan (Figure 3). Here scattered basalt boulders on the southern flank of Mt. Callahan overlie ancestral Colorado River gravels at ~1100 m above the modern river (Berlin, 2009). Boulders from the deposit are similar in age (~9.17 Ma; Berlin, 2009) to flows on Battlement Mesa (~9.3 Ma; Berlin, 2009) and are interpreted to represent debris-flow deposits derived from these units and shed northward into the ancient Colorado River valley (Berlin, 2009). Because these deposits have been transported across the axis of the canyon, ~1100 m represents a minimum value of incision (Berlin, 2009). The average modern transport slopes of debris-flow fans along the northern flank of Battlement Mesa (~0.07; Berlin, 2009) and the distance from Mt. Callahan to the present day position of the Colorado River (~4-5 km) imply that there may have been up to ~280-350 m of additional relief. Thus, it seems likely that incision in the vicinity of Mt. Callahan and Battlement Mesa is in the range of ~1380-1450 m. This value is consistent with estimates (~1400 – 1500 m) derived from the projection of Tertiary strata across the canyon from Battlement Mesa to the Roan Plateau (e.g., Bostick and Freeman, 1984). Collectively, these observations imply that an ancestral Colorado River was established across the western slope of the Rockies by ~10 Ma (e.g., Aslan et al., 2010) and that the river has subsequently incised ~1400-1500 m since that time.

Upstream of Glenwood Canyon (Figure 3), extensive preservation of ca. 10 Ma basalt flows at similar elevations (3000 - 3400 m) along the Colorado River suggest the presence of a broad, low relief erosional and/or transport surface prior to ~10 Ma (e.g., Larson et al., 1975; Kunk et al., 2002). Incision into this surface was probably ongoing by ~8 Ma, as suggested by relationships between basalt flows and fluvial gravel at Spruce Ridge and Little Grand Mesa (Kunk et al., 2002). Moreover, Kunk et al. (2002) suggest that the presence of a young, 3.03 +/-

0.02 Ma, high-elevation basalt at Gobbler's Knob (Figure 3), ~730 m above the modern Colorado River, records an increase in the rate of incision during the past ~ 3 Ma. However, the base of the basalt flow at Gobbler's Knob is unexposed, and is not known to be associated with river gravels (Kunk et al., 2002). Thus, the flow may have been emplaced significantly above the ancestral Colorado River ca. 3 Ma and may not directly constrain incision (Aslan et al., 2010). Irrespective of this debate over the pace of incision through time, it is clear that incision in the upper Colorado River near Glenwood Canyon postdates ~10 Ma, similar to the river near Grand Junction. The total amount of incision, however, may be somewhat lower with estimates ranging from ~750 m to perhaps ~1200 m (Table 1).

One of the primary tributaries of the upper Colorado River, the Gunnison River, displays a pronounced knickzone in the Black Canyon region (Sandoval, 2007; Aslan et al., 2008; Darling et al., 2009; Donahue et al., 2013). Abundant exposures of a strath terrace level that contain the ~0.64 Ma Lava Creek B tephra (Lanphere et al., 2002) reveal spatial differences in incision rate across this knickzone. Downstream of the Black Canyon, incision rates are ~150 m/Ma (Sandoval, 2007; Aslan et al., 2008; Darling et al., 2009). These rates increase within the Black Canyon to ~400-550 m/Ma (Sandoval, 2007; Aslan et al., 2008), but decrease again upstream to ~90 m/Ma above the knickzone (Sandoval, 2007; Aslan et al., 2008). Thus, the Black Canyon knickzone is clearly a prominent expression of transient incision along this system that may be related to the abandonment of Unaweep Canyon by capture of the Gunnison River (e.g., Hansen, 1987; Donahue et al., 2013; Aslan et al., in press).

***Green River System***

In contrast to the reasonably well-understood history of incision along the upper Colorado River, relatively little is known regarding the timing and magnitude of incision along the western slope of the Rockies in northern Colorado. Here, the White, Yampa and Little Snake rivers are not entrenched in narrow canyons for long reaches, and deposits of ancient fluvial gravels are exceedingly rare. However, the region was the locus of sediment accumulation during Oligocene through Miocene time (Kucera, 1962; Buffler, 1967; Buffler, 2003; Izett, 1975; Larson et al., 1975; McMillan et al., 2006), and these deposits, collectively referred to as the Browns Park Formation (Figure 4) (originally described by Powell, 1876 and summarized by Kucera, 1962 and Buffler, 2003), have been deeply incised and eroded by the modern drainage system. Thus, the degree of preservation of basin sediments allows for a minimum estimate of both the timing and magnitude of mass removed by fluvial activity (e.g., McMillan et al., 2006).

Regionally, the Browns Park Formation is exposed in the Elkhead Mountains in the northeast, the Flat Tops in the south, and along the Browns Park graben in the west (Figure 4). There are two, informally defined, members of the Browns Park Formation; a lower basal conglomerate that rests unconformably on older strata and an upper sandstone (Buffler, 2003). The basal conglomerate is generally thin (<100 m) but thickens and becomes coarser grained toward the margins of the basin; this unit is interpreted to represent alluvial fans being shed westward from the Park and Sierra Madre Ranges towards the Sand Wash Basin (Buffler, 2003) and may be correlative with deposits elsewhere referred to as the Bishop Conglomerate (Boraas and Aslan, 2013). The upper sandstone of the Browns Park Formation, in contrast, ranges up to ~670 m thick and consists of sandstones of both eolian and alluvial origin (Buffler, 2003). Paleocurrent indicators in these sandstones suggest transport directions toward the NNE (Buffler, 1967, 2003).

The age range of the Browns Park Formation is relatively well known from intercalated tuffaceous deposits; these range from ~24.8 Ma near the base of the sandstone member to ~8.2 Ma near the top of present exposure (Izett, 1975; Luft, 1985; summarized by Buffler, 2003). At City Mountain (Figure 4, Locality 3), a latite porphyry intruding the formation has been dated to 7.6 +/- 0.4 Ma (Buffler, 1967). Additionally, a volcanic tuff near the top of the Browns Parks along Vermillion Creek (Figure 4, Locality 4) has been dated at 9.8 +/- 0.4 Ma (Naeser et al., 1980). Collectively, these data suggest that sediment accumulation in the region continued from ~ 24 – 8 Ma.

Of particular relevance to this study are basalt flows that cap mesas and buttes throughout the region and often overlie thick sections of Browns Park Formation (~400-600 m - Buffler, 1967, 2003). The age of the uppermost Browns Park Formation is similar to the flows themselves (K-Ar ages ranging from 9.5 +/- 0.5 Ma to 10.7 +/- 0.5 Ma - Buffler, 1967, 2003). As these flows overlie the Browns Park Formation, they are broadly consistent with a minimum age for the formation of ~8-10 Ma (Buffler, 2003). Field relationships suggest, however, that local relief generation during fluvial incision likely post-dates basalt emplacement, and thus we pursued refined chronology from selected localities in the region.

**New Constraints on Late Miocene Incision in Northern Colorado**

In order to refine our understanding of the switch from deposition of the Browns Park Formation to incision along modern rivers, we supplement existing chronology with new $^{39}Ar/^{40}Ar$ ages from basalt flows. Localities were carefully chosen where local relationships between the timing of deposition and emplacement between volcanic units allowed us to reconstruct the magnitude of incision along primary rivers or their tributaries. Generally, these localities are characterized by basalt flows that cap mesas and represent a formerly continuous flow or sequence of flows that has been dissected by incision along modern rivers (Figure 5). In a few cases, where flows are absent, we use the exposed thickness of the Browns Park Formation where the uppermost strata are well dated by interbedded tuffs or intrusions that place bounds on the position of the ancestral land surface. Because ancestral river gravels are not preserved in these localities, our results do not constitute a measure of fluvial incision *sensu stricto* (Burbank and Anderson, 2011). Rather, they provide conservative estimates for the amount of relief generated in the landscape during fluvial incision.

The region has experienced extensional faulting in late Miocene time (e.g., Kucera, 1962; Buffler, 1967). Although fault slip is generally limited to a few hundred meters, displacement could have led to disruption of formerly-continuous basalt flows. Therefore, we confine our analysis to markers of incision within a given fault block. At each locality, we compare our results to the local thickness of preserved Miocene basin-fill sediments (Table 2). Because the upper member of the Browns Park Formation is typically sub-horizontal, the exposed vertical thickness of the Browns Park Formation provides a minimum bound on fluvial incision. Our analyses utilize USGS 1 x 2 degree quads (Tweto, 1976), the geologic map of Wyoming (Love and Christiansen, 1985) and modern National Elevation Dataset topographic data. A summary of results is shown in Table 2 and detailed $^{39}Ar/^{40}Ar$ methods, data, and results can be found in Appendix 1.

### *Elkhead Mountains Region*

The Elkhead Mountains represent a significant area of late Tertiary volcanism and comprise high topography near the Colorado/Wyoming border (Figure 4). The northern flanks of the range are drained primarily by the Little Snake River whereas the southern portions of the range lie within the Yampa River watershed. Late Tertiary volcanics of the Elkhead Mountains intrude and overlie the Browns Park Formation (Buffler, 2003) and form elevated mesas ideal for reconstructing the amount of post-incision relief. Of importance to this study, late Cenozoic extensional faulting is documented in the region and displacement across graben-bounding faults (Figure 6) may be on the order of ~300 – 600 m (Buffler, 1967).

***Battle Mountain, Squaw Mountain, and Bible Back Mountain.*** Basalt flows cap the Browns Park Formation in three locations north and south of the Little Snake River (Figure 6).

Atop Battle Mountain, the basal contact of these flows is exposed in a recent landside; the underlying Tertiary strata contain two thin, ~0.5 m thick, tuffaceous layers. The elevation of the flow base is ~2680 m and stands ~650 m above the elevation of the Little Snake River. We determined a $^{40}Ar/^{39}Ar$ age of 11.46 +/- 0.04 Ma of the basalt flow which is consistent with the older K-Ar age of ~11 Ma (Buffler, 2003).

Squaw Mountain sits directly across the Little Snake River southeast of Battle Mountain (Figure 6). Here, basalts also cap the mesa, but their base is not exposed, complicating the interpretation of whether these outcrops represent extrusive flows. Outcrops are non-vesiculated, free of significant phenocrysts and evidence for an intrusive or extrusive origin is equivocal. However, exposed just below the base of the outcrop are deposits of a volcanic breccia that is typically associated with extrusive flows elsewhere in the region (Buffler, 1967). These volcanic breccia deposits suggest a local surface vent, and we follow Buffler (1967) in considering the deposits atop Squaw Mountain as extrusive. The exposed thickness of the probable flow atop Squaw Mountain is ~20 m. We obtained a new $^{40}Ar/^{39}Ar$ age on the lowest exposure found of 11.45 +-/- 0.04 Ma, which overlaps in age with the age of the flow at Battle Mountain. The lowest exposure is at an elevation of ~ 2550 m and sits ~520 m above the modern elevation of the Little Snake River.

Overall, the basalt flows at Battle Mountain and Squaw Mountain lie directly across the Little Snake River from one another (Figure 6), are of essentially identical age, and are at broadly similar elevations. The relationship of these two basalt flows to the Little Snake River thus provides an opportunity for estimating the magnitude of fluvial incision along the Little Snake directly. Here, we assume that the ca. 11.5 Ma land-surface extended between Battle Mountain and Squaw Mountain. Taking the average elevation of the two flow bases, ~ 2600 m, above the modern elevation of the Little Snake, ~2030 m, yields an estimate of fluvial incision of ~580 m since ca. 11.5 Ma. This direct reconstruction of fluvial incision is similar to the exposed thickness of Browns Park Formation along the Little Snake and Yampa Rivers.

At Bible Back Mountain (Figure 6), the base of ~10 m thick, columnar jointed, flow is exposed on the southern flank of the peak. Here, it appears that there may be a second flow of similar thickness above this outcrop, but the nature of the exposure made this upper outcrop inaccessible. We obtained a new $^{40}$Ar/$^{39}$Ar age of the basal flow outcrop of 11.46 +/- 0.04 Ma (Table 2). The elevation of the flow base is ~2550 m and sits ~550 m above the modern Little Snake River. Map relations suggest that volcanic material is present at lower elevation toward the northwest; as mapped by (Buffler, 1967); these deposits are discontinuous remnants and probably represent debris downslope of the unit. The similarity of the amount of incision (~550 m) to that determined between Squaw and Battle Mountains above lends confidence that this is a relatively robust measure of the amount of relief generated during Miocene-Pliocene incision.

***Black Mountain and Mt. Welba.*** Geologic relationships between basalt flows in the southwestern Elkhead Mountains (Figure 6) show a markedly different relationship between the local thickness of Browns Park Formation and their elevation above the modern river. At Black Mountain, extensive deposits of vesiculated, basaltic debris cover the area adjacent to and directly below the mesa-shaped peak, but exposures are rare and the base of the flow (or sequence of flows) is not exposed. We sampled an outcrop on the northeast end of the main ridge and determined a $^{40}$Ar/$^{39}$Ar age of 10.92 +/- 0.16 Ma (Table 2), similar to ages from the eastern Elkhead mountains presented above. The lowest exposure of the flow is at an elevation of ~3160 m.

Nearby at Mt. Welba (Figure 6), exposures are also poor and difficult to access. There are three topographic peaks in the vicinity of Mt. Welba. Outcrops of volcanic deposits on the southernmost point, Mt. Oliphant, do not display definitive flow textures. However, at Mt. Welba itself, we discovered outcrops of weathered, vesiculated basalt inferred to represent an upper flow surface. A sample from this exposure yielded a new $^{40}Ar/^{39}Ar$ age of 12.60 +/- 0.06 Ma (Table 2). The lowest exposure of the flow is at an elevation of ~3150.

The flows at Black Mountain and Mount Welba are ~500 m higher in elevation than Battle Mountain yet sit atop a slightly thinner section of Browns Park Formation. If we project these elevations to the main valley of the Little Snake River, this would predict ~1170-1180 m of relief, far in excess of the ~350-400 m thickness of Brown's Park Formation exposed at these localities (Figure 6). However, the flows at Black Mountain and Mount Welba sit in the footwall block of a NW-trending normal fault system (Figure 6), and the possibility of syn- or post-depositional displacement along this structure (Buffler, 1967, 2003) makes projection to the Little Snake River subject to significant uncertainty. Rather, we take a more conservative approach of projecting to the nearest tributary within the same fault block, Slater Creek and Elkhead Creek, respectively (Figure 6); both with headwater elevations at ~2500 m. This yields local estimates of incision that are 660 m and 650 m from Black Mountain and Mt. Welba, respectively. The similarity of these values to the exposed vertical thickness of Brown's Park Formation suggests these are a likely measure of relief generation during fluvial incision.

***Sand Mountain.*** A thick (> 500 m) section of Brown's Park formation is mapped in the southeastern Elkhead Mountains (Snyder, 1980). The upper ~300 m of the formation is well-exposed in a landslide scar along the eastern flank of Sand Mountain (Figure 6). Here, a sequence of tuffaceous deposits were dated by (Snyder, 1980); ages range from ~12 Ma near the base of the section to 9.2 ± 1.7 Ma at the top. The section is capped by andesitic deposits that form the mesa-like summit of Sand Mountain proper; portions of these deposits have been alternatively interpreted as extrusive (Buffler, 1967) and intrusive (Snyder, 1980).

We re-evaluated these relationships along the eastern flanks of Sand Mountain and observed local relationships that support both interpretations. Beneath the summit, andesite is found at similar elevations to horizontal strata of the upper Browns Park Formation on either sides of a steep gully, suggestive of a sub-vertical, intrusive contact. But, we also discovered outcrops of porphyritic andesite with weak flow banding that overlie the section on the northeastern shoulder of the peak. These relationships lead us to conclude that the andesite is likely a shallow intrusion that has extrusive facies along the flanks of Sand Mountain. We dated a population of 15 individual sanidine crystals concentrated from a sample of the extrusive facies. These exhibited individual ages ranging from ~28 – 9 Ma (see Appendix 1). The youngest three samples cluster around 9 Ma; a weighted mean from these three crystals is 9.05 ± 0.04 Ma (Appendix 1 – Figure A-5)). We consider this a best estimate for the age of the volcanic deposit as the older crystals were likely xenocrystic and entrained during emplacement and/or flow of the andesite.

This age places a minimum bound on the age of the Browns Park Formation at Sand Mountain. Our results are consistent with the older fission-track age of the uppermost tephra in the deposit (9.2 ± 1.7 Ma; Snyder, 1980) but provide a more precise age. Notably, the Browns Park Formation must have been present for the intrusive relationships described above. However, we consider it likely that parts of the andesite were extruded on top of the Tertiary strata, and, thus, that the present exposures of the Browns Park Formation represent most of the pre-incision thickness. Locally, these inferences imply that fluvial incision and erosion into the Sand Wash basin did not begin until sometime subsequent to ~9 Ma. The exposed thickness of Browns Park sediments in the region implies that exhumation of material from this portion of the Sand Wash basin was at least 500 – 600 m, consistent with our estimates of incision from other parts of the Elkhead Mountains.

### *Flat Tops Region*

Near the headwaters of the Yampa and White Rivers (Figure 4), a laterally expansive sequence of at least 27 stacked basalt flows make up the large, high-elevation mesas for which the Flat Tops Range is named (Larson et al., 1975). Here, basalt flows comprise an overall thickness of ~470 m and range in age from approximately 24 to 9.6 Ma (Larson et al., 1975; Kunk et al., 2002). Individual flows range in thickness from 3 m to ~60 m where locally ponded against paleo-topography (Larson et al., 1975). In the southwest of the range, most of the stratigraphy is composed of superposed flows, which become increasingly intercalated with the Browns Park Formation toward the northeast (Figure 7), in the direction of the Yampa River Valley and the Park Range (Figure4). Overall, the sequence of stacked basalt flows are relatively conformable and lie within a several hundred meters elevation from one another, despite the wide range in age from ~24 – 10 Ma (Larson et al., 1975). This relationship suggests that basalts were likely extruded onto a low relief surface that persisted in the Flat Tops region until ~10 Ma. Thus, we follow Larson et al. (1975) in inferring that present day canyons that dissect formerly continuous flows provide a measure of incision subsequent to that time.

We estimate the amount of fluvial incision in the uppermost headwaters of the Yampa and White Rivers by averaging the highest elevation of the basalt surface on both sides of the modern valley and subtracting the elevation of the modern river channel. Across most of the Flat Tops region, the highest interfluves are capped by ca. 20 Ma basalt flows (Larson et al., 1975), but a few mapped flows that cap the highest peaks (Derby Peak, W Mountain, Sugarloaf Mountain – Figure 7) range from ~15 Ma to as young as 9.6 ± 0.5 Ma (Larson et al., 1975). Although the former extent of all of these flows is uncertain, their presence on the flanks of the volcanic pile that comprises the Flat Tops (Figure 7) suggests that the present-day relief must have developed subsequent to their deposition. Thus, we consider ~10 Ma as a reasonable bound on the timing of local relief generation in the upper tributaries of the White and Yampa Rivers.

In the headwaters of the White River (A-A', Figure 7) from Lost Lakes Peak to Sable Point, it appears that there has been ~ 900 m of fluvial incision in the last 9.6 +/- 0.5 Ma. In the headwaters of the Yampa River (B-B', Figure 7) from Orno Peak to Flat Top Mountain, the magnitude of incision appears to be somewhat less, ~ 700 m, but still greater than observed in the Elkhead Range.

***Yampa River Valley***

The third region we studied is in the headwaters of the Yampa River, north and east of the Flat Tops range (Figure 4). Near the town of Yampa, CO, the river flows north in a fault bounded valley before making a series of sharp bends; east towards Woodchuck Mountain, north parallel to the flank of the Park Range (Figure 8) and eventually west at Steamboat Springs, CO (Figure 4). Along much of its course, the river flows in Cretaceous Mancos Shale and the overlying Browns Park Formation, both of which have been intruded by young dikes and volcanic plugs (e.g., Kucera, 1962).

***Lone Spring Butte.*** In the western half-graben, a ~10 m thick, porphyritic, flat-lying basalt flow with moderately well-developed flow banding is exposed atop Lone Spring Butte (Figure 8). In hand sample, the basalt has phenocrysts of olivine, plagioclase, and mafic accessory minerals. The base of the flow is at an elevation of ~3090 m, ~640 m above the modern Yampa River. This flow unconformably overlies gently dipping coarse boulder conglomerates of the basal Browns Park Formation. Boulders up to ~1 m in diameter are composed of crystalline gneisses and granites, similar to those exposed in the Park Range east of the valley (Figure 8; Kucera, 1962). Bedding within the deposit dips ~20-25° west and appears to have been tilted in the footwall of an east-dipping normal fault, which defines the Yampa Valley half graben (Figure 8). Volcanic ash from a thin Browns Park deposit overlying the basal conglomerates has a zircon fission track age of 23.5 +/- 2.5 Ma (Izett, 1975; Luft, 1985), confirming that the underlying conglomerate represents the base of the formation.

Deposits of volcanic breccia, previously described by Kucera, (1962) and Buffler, (1967), are also exposed along the flank of Lone Spring Butte, ~300-400 m below the base of the basalt flow. Similar deposits are present locally throughout the Yampa River valley and were termed the Crowner Formation Kucera, (1962); herein we simply refer to these as 'Crowner deposits'. At Lone Spring Butte these deposits consist of poorly sorted, subangular to angular, cobbles of volcanics mixed with lithic fragments of Browns Park Formation, Mancos Shale, and granitic clasts derived from the Browns Park basal conglomerate. Crowner deposits are thin to thick bedded, and individual beds are on the order of a meter thick. The bedding is generally horizontal planar although there is a minor amount of small-scale cross bedding in sandier facies. Cobble- to pebble-rich facies are poorly sorted and massive. Crowner beds dip concentrically inward in a ring-like geometry. Collectively, these observations suggest that the Crowner deposits represent maar deposits developed during phreatomagmatic interaction of volcanic intrusions into ground-water saturated Browns Park Formation sandstones (Buffler, 1967). Thus, it is possible that these units were deposited close to the position of the ancestral-land-surface along the flank of Lone Spring Butte.

We sampled several of these volcanic units for $^{39}Ar/^{40}Ar$ chronology. A sample from the basalt flow capping the mesa of Lone Spring Butte yielded a $^{40}Ar/^{39}Ar$ age of 6.15 +/- 0.03 Ma (Table 2). The relatively thin exposure of Browns Park Formation (~80 m) preserved between the tuff (~23.5 Ma) and the basalt flow (~6 Ma) seems to suggest that a significant amount of sediment was removed by erosion prior to the emplacement of the basalt flow atop Lone Spring Butte.

We also dated samples that constrain the age of the Crowner deposits at Lone Spring Butte. A basaltic clast, contained within bedded Crowner deposits yielded an $^{39}Ar/^{40}Ar$ age of 7.0 +/- 0.4 Ma, consistent with the eruptive age of the basalt flow. We also obtained a younger age of 4.62 +/- 0.05 Ma from an intrusive dike that cross-cuts bedded Crowner deposits. Notably, all three of these ages attest to a significant episode of volcanism at ca. 7 – 5 Ma in the present-day

Yampa River valley, consistent with recent age determinations on relict volcanic necks in the region (Cosca et al., 2014).

Relationships between deposits at Lone Spring Butte and the underlying Browns Park Formation make determination of the timing and amount of fluvial erosion difficult in this locality. The base of the 6.15 ± 0.03 Ma flow atop Lone Spring Butte sits ~630 meters above the Yampa River (Figure 8), and a simple interpretation would suggest that all of this relief postdates ca. 6 Ma. However, the presence of the angular unconformity between the base of the flow and the underlying Browns Park Formation suggests that there may have been significant erosion and removal of the upper Browns Park prior to ca. 6 Ma. Notably, if the Crowner deposits on the flank of Lone Spring Butte indeed represent a paleo-land surface, their present day position below the summit imply that a minimum of ~300-400 m of relief existed by ca. 6 Ma. Thus, although it is possible that incision did not begin until after 6 Ma in this locality, the relationships observed between the basalt flow atop Lone Spring Butte, the underlying ash, and the Crowner deposits make it seem likely that some erosion of the Browns Park began prior to ~ 6 Ma in the Yampa River Valley.

***Woodchuck Mountain.*** Toward the northeast, the Yampa River makes a sharp turn to the east and enters a second half-graben along the flank of the Park Range (Figure 8). Basalt flows are poorly exposed atop another butte named Woodchuck Mountain (Figure 8), but appear to be at least ~50 m thick. At the top of Woodchuck Mountain, the topography is expansive and approximately flat, suggesting the top of a flow surface. Here, a sample from a rubbly outcrop yielded a $^{40}Ar/^{39}Ar$ age of 6.04 +/- 0.04 Ma (Table 2). A second sample was collected from dark basalt outcrop with moderately developed flow banding approximately 65 m lower in elevation (~2620 m). This sample yielded a similar age of 5.97 +/- 0.06 Ma. The proximity of Woodchuck Mountain to the Yampa River and the presence of Browns Park Formation beneath the flow make this a robust site to estimate that ~460 m of relief has developed following basalt emplacement at ca. 6 Ma.

**Summary: Mio-Pliocene Differential Incision along the Western Slope**

Local relationships between volcanic deposits dated with new $^{39}Ar/^{40}Ar$ ages (Table 2) and the Browns Park Formation provide new constraints on the timing and magnitude of incision along northern rivers draining the western slope of the Rockies (White, Yampa, and Little Snake Rivers). Regionally, basalt flows capping the Browns Park Formation in the northern and western Elkhead Mountains require that fluvial incision along the Little Snake River began sometime after ~11 Ma. Given that the youngest ages obtained from the uppermost strata in the Brown's Park Formation are ~ 9 Ma at Sand Mountain (Snyder, 1980; Luft, 1985) and ~8.5-8.2 Ma in Browns Park proper (Izett, 1975; Naeser et al., 1980; Luft, 1985) it seems likely that incision probably began shortly after ~ 9 Ma. Similarly, the presence of ~10 Ma volcanic deposits atop modern interfluves in the Flat Tops range (headwaters of White and Yampa Rivers) suggest that incision post-dates ~10 Ma.

In the Yampa River valley proper, geologic relationships regarding the timing of incision are somewhat more complicated. The hiatus in time associated with the unconformity below Lone Spring Butte (~23 Ma to 6 Ma) implies that a significant, but unknown, amount of material could have been removed, perhaps related to tilting during extensional faulting (Buffler, 2003). However, whether this erosion occurred between ~9 – 6 Ma, as might be inferred from relationships described above in the Elkhead Mountains, or whether it occurred farther back in the Miocene, is unknown. As noted above, the presence of ~7 Ma clasts within the Crowner deposits that were transported at the surface implies that some topographic relief was present during the eruption of 5 – 7 Ma volcanics in the Yampa River Valley (e.g., Cosca et al., 2014). Unfortunately, we are unable to be place quantitative estimates on the amount of relief. Geologic relationships at Woodchuck clearly imply >400 m of post ~6 Ma incision. Thus, although it seems likely that the onset of incision across the region occurred prior to 6 Ma, it is also possible that incision did not initiate until as recently as ~6 Ma.

Regardless of the exact timing (6 - 9 Ma), our results suggest that the total amount of post ~10 Ma incision varies from north to south across the study area. Relationships in the Elkhead Mountains clearly indicate that incision post 10 Ma was limited to 550 – 650 m. In the Yampa River valley, adjacent to the Park Range, we see similar values (Figure 9). However, the amount of post 10 Ma incision appears to be somewhat greater in the Flat Tops, ranging up to ~900 m (Figure 9). All of these estimates are significantly lower than the ~1200 – 1500 m of incision known to have occurred along the upper Colorado River system during broadly the same time period (Figure 9).

## CHANNEL PROFILES ALONG THE WESTERN SLOPE

### Background

#### *Channel Profiles as a Guide to Landscape Forcing*

Analysis and interpretation of longitudinal profiles of bedrock channels that are actively incising into mountainous landscapes (e.g., Whipple, 2004), has become a relatively common tool to guide the interpretation of landscape evolution in erosional settings. Although these analyses are typically conducted in convergent mountain ranges where differential rock uplift is associated with permanent deformation of the crust (e.g., Seeber and Gornitz, 1983; Kirby and Whipple, 2001; Kirby et al., 2003; Wobus et al., 2006; Harkins et al., 2007; Ouimet et al., 2009; Merritts and Vincent, 1989; Snyder et al., 2000; Duvall et al., 2004; Safran et al., 2005; Kirby and Whipple, 2012), recent studies export these techniques to regions of long-wavelength, epiorogenic uplift (e.g., Karlstrom et al., 2012). Here, we use channel profile analysis to examine possible drivers of Miocene exhumation related to possible epiorogenic uplift along the western flank of the Rocky Mountains. We provide only a brief introduction to the techniques below, and the reader is directed to several reviews of the subject for a more comprehensive examination of this technique (Whipple, 2004; Whipple et al., 2012; Kirby and Whipple, 2012).

Channel profile analysis exploits the empirical scaling relation between the local channel gradient ($S$) and the contributing drainage area upstream ($A$). In graded channel profiles (Mackin, 1948) from mountain ranges around the world, channel slope follows an empirical relationship of the form,

$$S = k_s A^{-\theta}, \quad (1)$$

where $k_s$ is a measure of the relative channel steepness, termed the 'channel steepness index', and $\theta$ is the 'concavity index', a measure of how rapidly slope varies with changes in contributing drainage area (e.g., Flint, 1974; Snyder et al., 2000). In practice, the steepness index ($k_s$) and concavity index ($\theta$) can be determined by linear regression of slope ($S$) against drainage area ($A$) in log-log space. However, small uncertainties in the slope of this regression ($\theta$) yield large variations in the regression intercept ($k_s$) (Wobus et al., 2006). Thus, several methods for determining a normalized gradient index have been proposed to surmount this influence (e.g., Sklar and Dietrich, 1998; Wobus et al., 2006; Perron and Royden, 2013; Royden and Perron, 2013). Here we follow a large body of work (e.g., Kirby and Whipple, 2012) that determines a normalized channel steepness ($k_{sn}$) by using a fixed reference concavity ($\theta_{ref}$); this method has been shown to provide a reasonable comparison of channels with widely different contributing drainage areas (Wobus et al., 2006; Kirby et al., 2003).

Over the past decade, numerous studies demonstrate that the normalized channel steepness index ($k_{sn}$) co-varies with erosion rate in landscapes at or near steady-state (see review in Kirby and Whipple, 2012). Early in the development of the metric, studies were limited to steady-state landscapes where uplift rates were known from independent geomorphic markers (e.g., Snyder et al., 2000; Kirby and Whipple, 2001; Duvall et al., 2004). These results supported theoretical predictions (e.g., Whipple and Tucker, 1999) that the normalized channel steepness ($k_{sn}$) scales monotonically with rock uplift/erosion rate, but that the concavity index ($\theta$) is relatively insensitive to rock uplift/erosion rate, provided that rock uplift, substrate properties and climate were spatially uniform (e.g., Kirby and Whipple, 2001). . The success of early studies bolstered the use of channel profile analysis as a tool to determine spatial patterns of rock uplift (Wobus et al., 2006). In recent years, the application of cosmogenic isotopic inventories in modern sediment to measure basin averaged erosion rates (e.g., Bierman and Steig, 1996; Granger et al., 1996) has enabled comparisons of channel steepness ($k_{sn}$) and catchment-scale erosion rates (e.g., Safran et al., 2005; Harkins et al., 2007; Ouimet et al., 2009; DiBiase et al., 2010; Cyr et al., 2010; Bookhagen and Strecker, 2012). Thus, all other factors being equal, normalized channel steepness can provide a first-order measure of spatial patterns in differential rock uplift (Kirby and Whipple, 2012).

In practice, numerous additional factors influence the adjustment of river profile gradient to erosion rate. These include: variably resistant lithology (Moglen and Bras, 1995; Duvall et al., 2004; Pederson and Tressler, 2012), climatically forced spatial variations in discharge (Roe et al., 2002; Bookhagen and Strecker, 2012), the role of thresholds and temporal distributions of discharge events (Snyder et al., 2003; Tucker, 2004; Lague et al., 2005; DiBiase and Whipple, 2011), and adjustments in channel hydraulic geometry (Duvall et al., 2004; Finnegan et al., 2005; Wobus et al., 2008). All of these factors may result in a non-linear scaling between channel steepness and erosion rate (Lague et al., 2005). Although global data compilations (Kirby and Whipple, 2012) suggest that variability among field sites likely reflects differences in substrate lithology and climate (DiBiasi and Whipple, 2011), within a given setting, it seems clear that that channels experiencing higher rates of erosion/rock uplift exhibit greater channel steepness ($k_{sn}$).

These scaling relationships also provide a means to interpret transient responses to perturbations in base level, either through drainage reorganization or variable uplift rate (e.g., Howard, 1994; Whipple and Tucker, 1999; Whipple and Tucker, 2002; Whittaker et al., 2007). Transient river profiles have been recognized in tectonically active landscapes around the world (e.g., Crosby and Whipple, 2006; Wobus et al., 2006; Harkins et al., 2007; Kirby et al., 2007; Berlin and Anderson, 2007; Whittaker et al., 2007; Whittaker et al., 2008; Cook et al., 2009; Olivetti et al., 2012; Morell et al., 2012). Interpretation of such landscapes can be guided by channel profile analysis. We follow Haviv et al. (2010) and Kirby and Whipple, (2012) as distinguishing between "vertical-step" knickpoints – those that form an isolated, steepened reach of a river profile – from "slope-break" knickpoints – those that separate two distinct reaches of a profile with different $k_{sn}$ values. The distinction is that the latter is expected to form in response to a sustained perturbation in forcing (Wobus et al., 2006), whereas the former is often an indication of features that are anchored to the river profile (i.e., an steepened reach across resistant substrate).

***Channel Steepness along the Western Slope of the Rocky Mountains***

Previous analysis of modern channel profiles draining the western slope of the Colorado Rockies provides motivation for the present study. In a regional scale analysis, Karlstrom et al. (2012) showed that channels in the upper Colorado River watershed that drain high topography above low-velocity mantle have higher normalized steepness indices ($k_{sn}$) than those that drain topography developed above mantle with higher seismic wave speeds in the Green River watershed (see Figure 3 of Karlstrom et al., 2012). Notably, this signal does not appear to reflect climatically induced variations in mean annual discharge; the scaling between discharge and drainage area in the upper reaches of the Colorado and Green River watersheds are quite similar (Darling et al., 2012). In fact, re-analysis of these channels by Pederson and Tressler (2012) utilizing historic discharge records shows effectively the same pattern (see Figure 5 of Pederson and Tressler, 2012). Thus, variations in channel steepness along the western slope are not simply an artifact of differences in discharge.

In the second part of our study, we seek to evaluate potential explanations for these variations in channel steepness. One explanation may involve differences in lithology; (Pederson and Tressler, 2012) suggest that variably resistant substrate is the dominant influence on the position of knickpoints along the Green-Colorado River system. They argue that knickpoints and knickzones are anchored to resistant substrate and act to 'decouple' topography from proposed loci of uplift (e.g., along the western edge of the Colorado Plateau, van Wijk et al., 2010). A second explanation may involve differences in the history of relative base-level fall, as upstream migration of knickpoints reflecting integration of the lower Colorado River (Cook et al., 2009; Darling et al., 2012; Pederson et al., 2013) may have influenced both patterns of incision and channel steepness across portions of the drainage network. Because these rivers may not be in steady state (e.g., Berlin and Anderson, 2007), we seek to identify transients in the system that may be associated with variations in channel steepness and distinguish these from knickpoints that are anchored to locally resistant substrate (e.g., Pederson and Tressler, 2012).

Finally, we compare patterns of channel steepness to the spatial distribution of post-10 Ma incision across the western slope of the Colorado Rockies. We ask whether the observed patterns are consistent with those expected by an increase in erosivity (e.g., Wobus et al., 2010) or a change in base level (e.g., Pederson et al., 2013), or whether regional patterns require a component of tilting associated with buoyant mantle beneath the Colorado Rockies.

**Channel profile analysis**

We determine normalized channel steepness values ($k_{sn}$) for six of the major rivers draining the western flank of the Rockies: the Colorado, Gunnison, and Dolores Rivers, and the White, Yampa, and Little Snake Rivers upstream of their respective confluences with the Green

River. Extraction of channel profiles and determination of channel steepness values follow the methods of Wobus et al. (2006); open-source codes are available at http://www.geomorphtools.org. Topographic data and upstream drainage area were extracted from a USGS 30m digital elevation model (DEM). To reduce noise associated with the pixel-to-pixel channel slope, elevation data were smoothed using a moving-average window of 1 km and channel slopes calculated over a fixed vertical interval of 12.192 m (equivalent to the 20 m contour interval of the original data used to generate the DEM).

Topographic data along the Colorado, Gunnison, and Dolores rivers contain artifacts that represent man-made reservoirs, the largest of which significantly influence local slope-area relationships along channel profiles (e.g., Karlstrom et al., 2012). The locations of these reservoirs were verified against a USGS database and were manually removed by linear interpolation of the channel elevation just upstream and downstream of each reservoir.

We analyzed topographic data along all six channels on log($S$)-log($A$) plots and used linear regression to determine values of $k_{sn}$ along each channel (c.f., Wobus et al., 2006). A reference concavity ($\theta_{ref}$) of 0.45 was used for all $k_{sn}$ analyses in this study. We calculated steepness indices ($k_{sn}$) across a fixed interval along each channel of 0.5 km. We binned these measurements every 10 km and calculated the mean and standard deviation. The average $k_{sn}$ value for each bin then provides a measure of 'local normalized channel steepness', or 'local $k_{sn}$', at a spacing of 10 km and the standard deviation provides an estimate of the error for each bin . This approach allowed for an objective measure of channel steepness that is not tied to a choice of regression interval (e.g., Kirby and Ouimet, 2011) and facilitated comparison to reaches of the channels underlain by variable lithology.

Bedrock geology along rivers in the study area was extracted from the digital geologic maps of Colorado (Green, 1992; Tweto, 1979), Utah (Hintze et al., 2000; Hintze, 1980), and Wyoming (Green and Drouillard, 1994; Love and Christiansen, 1985) and divided into the map units shown in Figure 10. These allowed us to examine whether streamwise variations in channel steepness were tied to lithologic variations along the channel at length scales > 10 km (Figure 11 and Figure 12). To compare differences among channels, we evaluate the mean normalized steepness ($k_{sn}$) of reaches that are underlain by substrate with similar mechanical characteristics. We focus on two primary rock types – Tertiary sandstones, which include the Wasatch and Uinta Formations, as well as the Brown's Park Formation, and Cretaceous shales (Lewis and Mancos Formations). In a recent study of rock strength, Tressler (2011) found that variations in compressive strength among the former group are minimal. Compressive strength of Cretaceous shales was unable to be determined, due to the overall mechanical weakness of these units (Tressler, 2011), but we assume that variations across the study area are minimal. Therefore, comparison of channel steepness indices along these reaches should reflect differences in stream profile gradient that are irrespective of substrate erodibility.

**Results of Channel Profile Analysis**

***Colorado, Gunnison, and Dolores Rivers***

The profile of the Colorado River exhibits a broad increase in channel steepness along the central portion of the profile (Figure 11A). Generally, the lowest values of $k_{sn}$ (~20 – 40 $m^{0.9}$) are observed immediately upstream of the confluence of the Green River; $k_{sn}$ then increases toward values of ~90 – 100 $m^{0.9}$ just downstream of Glenwood Canyon (Figure 11A). The uppermost ~200 km of the profile are again gentler, with $k_{sn}$ ~60 – 70 $m^{0.9}$. Superimposed on this general trend, three locally elevated regions of $k_{sn}$ correlate with the position of distinct knickzones along the Colorado River at Westwater Canyon, Glenwood Canyon, and Gore Canyon (Figure 11A). The association of these knickzones with crystalline basement rocks and their limited spatial extent suggest that these steep reaches are likely anchored to the underlying bedrock lithology, consistent with the interpretations of Pederson and Tressler (2012). However, these local features do not explain the broader signal of steep reaches along the central ~300 km of the profile (Figure 11A).

In contrast to the Colorado, the channel profile of the Gunnison River is characterized by a prominent knickzone within the Black Canyon of the Gunnison, ~400-500 km upstream from the Colorado – Green confluence (Figure 11B). The reach of the river below the knickzone exhibits local $k_{sn}$ of ~60 $m^{0.9}$, consistent with the Colorado River downstream (Figure 11B). However, local $k_{sn}$ values within the knickzone are much greater, ranging up to ~770 $m^{0.9}$ (Figure 11B). Although the steep reach within Black Canyon of the Gunnison is developed within Precambrian crystalline rocks, similar to those along the Colorado River, recent analysis of incision rates along this portion of the channel network suggest that this knickpoint is associated with spatial differences in incision rate that suggest that this feature represents an upstream migrating wave of incision (Sandoval, 2007; Darling et al., 2009; Donahue et al., 2013). Although it is possible that the knickpoint is linked to autogenic drainage reorganization along the Colorado River network (Aslan et al., in press, it probably also reflects the influence of resistant lithology in retarding regional incision. Because this knickpoint complicates interpretation of $k_{sn}$ values, we do not attempt a direct comparison with channel steepness along other rivers.

Directly upstream from its confluence with the Colorado River, the Dolores River displays variable, but still relatively high values of local $k_{sn}$ (Figure 11C). These high values of local $k_{sn}$ near the confluence may suggest adjustment of the Dolores River to base level lowering along the Colorado River or the influence of variable substrate (the Dolores flows through the Permian Cutler sandstone and the Morrison Formation through this section). Much of the profile, however, exhibits local $k_{sn}$ values between ~30 – 60 $m^{0.9}$. A prominent knickpoint occurs in the headwaters ~450 km above the confluence with the Green River (Figure 11C). Because data on the timing and magnitude of incision are sparse along the Dolores River, we are unable to evaluate whether this feature is transient, similar to the Black Canyon of the Gunnison, or whether this has developed above resistant Paleozoic/Mesozoic substrate (Figure 10 and Figure 11C). For these reasons, we exclude the Dolores from further discussion.

***Yampa, White and Little Snake Rivers***

The White, Yampa and Little Snake rivers are all tributaries of the Green River that drain the western slope of the northern Colorado Rockies (Figure 2). Because the Little Snake River is itself a tributary of the Yampa, we discuss these profiles together. The lower reach of the Yampa River, between the confluence of the Little Snake and the Green Rivers, coincides with Dinosaur Canyon (Figure 11E) where the river flows through the eastern tip of the Uinta block (Hansen, 1986). Within this reach, values of local $k_{sn}$ are generally high (100-150 $m^{0.9}$) and exhibit rather substantial scatter (Figure 11E). Rocks of the Uinta Mountain Group are typically quite resistant and probably contribute to the steepening of the river profile, either directly (Pederson and Tressler, 2012) or through the input of coarse debris from canyon walls (Grams and Schmidt, 1999). In addition, this region is a locus of late Cenozoic faulting (Hansen, 1986), and it is possible that the profile may be influenced by young or ongoing deformation. Alternatively, the Dinosaur Canyon knickzone may represent a transient feature associated with integration of the Green River into the Colorado River watershed, an event that is thought to have occurred between ~8 Ma and ~2 Ma (Hansen, 1986; Darling et al., 2012).

The Little Snake River joins the Yampa River just upstream of Dinosaur Canyon, and along most of its reach the profile is characterized by relatively uniform values of normalized channel steepness (Figure 11D). A singular exception to this occurs in the headwaters, approximately ~310 km above the confluence with the Green River, where a locally steep reach occurs in crystalline basement (Figure 11D). . Similar to knickpoints along the Colorado River, this knickpoint is characterized by a localized steepening of the profile, and $k_{sn}$ values both upstream and downstream are similar (Figure 11D). Thus, we interpret this feature as anchored to resistant bedrock. Overall, the morphology of the Little Snake profile above Dinosaur Canyon appears to be consistent with a graded, or equilibrium, profile.

Upstream of Dinosaur Canyon, the Yampa River displays also relatively uniform values of local $k_{sn}$ along most of its profile. There is, however, a notable increase in $k_{sn}$ toward the headwater reaches of the river (Figure 11E). There are two possible explanations for this increase in channel steepness in the headwaters. First, the river heads in the basalt fields that comprise the Flat Tops, and it seems possible that profile steepening may be associated with abundant coarse debris shed from this range (Larson et al., 1975). However, the headwater region of the Yampa also overlies the western flank of the region of anomalously low P-wave velocity (Figure 2), and so it is also possible that these steepened reaches reflect long-wavelength tilting associated with this feature.

The White River exhibits a remarkably smooth profile with no obvious knickpoints (Figure 11F). Although local $k_{sn}$ remains relatively uniform for ~200 km upstream of the junction with the Green River, $k_{sn}$ values broadly increase toward the uppermost headwaters of the White River (Figure 11F) from values ~ 40 $m^{0.9}$ to nearly ~100 $m^{0.9}$. Again, whether this steepening is associated with coarse debris being shed off of the Flat Tops, or whether it is a signal of differential uplift between the headwaters and the Green River remains uncertain. We will address this question further in the regional discussion below.

**Summary: Lithologic influences on profile steepness**

One of the notable results of this study is that systematic changes in channel steepness along the western slope do not appear to be controlled by differences in lithology. The lower reach of the Colorado in the study area is relatively steep ($k_{sn}$ = ~90 – 100 $m^{0.9}$), whereas the Little Snake is significantly gentler ($k_{sn}$ = ~40 $m^{0.9}$). The White ($k_{sn}$ = ~80 $m^{0.9}$) and Yampa ($k_{sn}$ = ~70 $m^{0.9}$) Rivers are intermediate in both geographic distribution and normalized steepness. These differences persist when we restrict our analysis to lithologies with broadly similar mechanical characteristics. The Colorado River exhibits relatively high values of $k_{sn}$ where it flows across Tertiary sandstones equivalent to the Browns Park ($k_{sn}$ = 81.6 +/- 38.5 $m^{0.9}$), within the Wasatch Formation ($k_{sn}$ = 107.3 +/- 39.0 $m^{0.9}$), and, notably, within the Mancos Shale ($k_{sn}$ = 82.6 +/-14.8 $m^{0.9}$) (Figure 12). In contrast, the profile of the Little Snake River is approximately half as steep within the Browns Park and equivalent sediments ($k_{sn}$ = 36.8 +/- 0.1 $m^{0.9}$), and nearly three times less steep within the Wasatch Formation ($k_{sn}$ = 36.5 +/- 6.6 $m^{0.9}$). Although there is significant variability, channel steepness values along the White and Yampa Rivers are intermediate between these end members. This analysis provides compelling evidence that substrate lithology is not the dominant control on variations in channel steepness across the study area. Rather, north-south variations in channel steepness appear to correlate strongly with the magnitude of Late Cenozoic incision along the western slope (Figure 12), a point that we address in our regional interpretations.

Exceptions to the absence of a regional correlation between steepness and lithology occur within reaches of crystalline Precambrian rocks, in the Flat Tops region, and within Dinosaur Canyon along the Yampa River. Along the Gunnison, Colorado, and Little Snake Rivers, reaches underlain by crystalline bedrock often coincide with isolated knickpoints that are associated with locally elevated $k_{sn}$ values. As noted above, we interpret these correlations as indicative of locally resistant substrate (e.g., Tressler, 2011; Pederson and Tressler, 2012) and exclude them from our regional analysis. Likewise, the knickzone along the Yampa River through Dinosaur Canyon (Figure 11E and Figure 9) was also excluded from regional comparison. Here, locally resistant substrate (e.g., Darling et al., 2009; Pederson and Tressler, 2012), input of coarse debris (Grams and Schmidt, 1999) or ongoing late Cenozoic faulting (Hansen, 1986) all have the potential to influence channel steepness along this reach. Finally, because of the potential for localized steepening associated with coarse debris being shed off of the Flat Tops (Larson et al., 1975), we consider the steep profiles along the uppermost ~50 km of the Yampa and White Rivers as uncertain in origin.

## POTENTIAL DRIVERS OF LATE MIOCENE INCISION

Late Cenozoic climate change (e.g., Wobus et al., 2010), base-level fall during drainage basin integration (Pederson et al., 2013), and differential rock uplift in the Rocky Mountain headwaters (Karlstrom et al., 2012) have all been proposed as possible drivers of late Miocene exhumation along the western slope of the Colorado Rockies. The combination of new constraints on the timing and magnitude of fluvial incision and channel profile analysis presented here demonstrate that 1) the onset of fluvial incision is broadly synchronous at ca. 6-9 Ma along tributaries of the Green and Colorado River systems, 2) channel profile steepness ($k_{sn}$) of major river systems increases from north to south along the western slope (Figure 12), 3) differences in profile steepness are independent of both average annual discharge (cf., Pederson and Tressler, 2012) and substrate lithology (Figure 12), and 4) the steepest rivers have experienced the greatest amount of late Cenozoic incision (Figure 12). In this section, we consider what potential driving mechanisms best explain the correspondence of steep channels and deep incision across the study area.

### Enhanced Fluvial Incision in the Late Cenozoic

One of the potential explanations for late Cenozoic incision along the western slope of the Rockies is the possibility that climatic changes during the late Miocene enhanced the potential for fluvial transport, either through an increase in storminess (e.g., Molnar, 2001, 2004) or increased mean discharge from snowmelt (Pelletier, 2009). Apparent increases in global sedimentation rates between 3-5 Ma have often been cited as evidence for an increase in the efficacy of fluvial erosion (e.g., Zhang et al., 2001; Kuhlemann et al., 2002), although the global significance of these findings have recently been called into question based on isotopic archives (Willenbring and von Blanckenburg, 2010).

Along the western slope, evidence for an increase in incision rate is limited, however. Along the Colorado River, the key marker often cited as evidence for an increase in Pliocene incision rates is the basalt flow at Gobbler's Knob (Kunk et al., 2002). As argued previously by Aslan et al. (2010), the absence of fluvial gravels means that relationship of this flow to the position of the river is uncertain. In contrast, if one considers the ca. 640 Ka Lava Creek B tephra and basalt flows of known association to the position of river gravels and inset fluvial terrace/fan complexes, incision rates along the Colorado River appear to be relatively constant with time (Aslan et al., 2010). Likewise, incision data from the Gunnison River permit semi-steady long term differential incision over the last 10 Ma above and below the Black Canyon knickpoint (Donahue et al., 2013). Along northern rivers, markers of younger age are sparse, but the data admit the possibility of relatively constant incision during the past ~6 - 9 Ma. Although it is possible that slightly elevated rates of incision during past ca. 640 Ka (Dethier, 2001) reflect a climatic influence, these rates are only subtly different from post ~10 Ma averages (Aslan et al., 2010). Thus, we consider the question of whether incision rates increased during Pliocene time as yet unanswered along the western slope of the Colorado Rockies.

Regional patterns in the magnitude of fluvial incision and channel steepness, however, argue strongly that climate change is not a the primary driver of incision along the western slope. Nearly all models of river profile response to an increase in the efficiency of erosion (e.g., Wobus et al., 2010), regardless of whether this is associated with changes in mean discharge or storminess (e.g., Lague et al., 2005), are characterized by 1) a reduction of steady-state channel gradients that leads to 2) systematically greater incision in an upstream direction. (Whipple and Tucker, 1999; Wobus et al., 2010). These expectations are not met along the western slope. The Colorado River has experienced the greatest amount of incision in the last ~10 Ma, but yet remains the steepest of the rivers in our study area (Figure 12). Moreover, it seems unlikely that climate change alone can explain spatial variations in the amount of incision observed along the western slope. It is difficult to envision a change in erosive efficiency that could simultaneously drive ~1500 m of incision along the Colorado River while only resulting in ~500 m of erosion along the Little Snake River. These rivers are only a few hundred kilometers apart, have headwaters at broadly similar elevations, and exhibit similar discharge-area relationships today. Overall, the correlation of channel steepness with synchronous, yet spatially variable, fluvial incision appear to rule out climate change as a significant driver of incision in western Colorado; some additional process is required to maintain steep gradients in the face of ongoing incision.

**Transient Incision during Drainage Integration**

Relative base level fall during drainage integration has long been thought to be a primary driver of incision and canyon development across the Colorado Plateau (Hunt, 1956; Pederson et al., 2002). Although the present position of Grand Canyon may exploit an older paleocanyon (e.g., Flowers et al., 2007; Wernicke, 2011; Flowers and Farley, 2012), or segments of preexisting canyons (Karlstrom et al., 2014), it seems clear that final integration of the Colorado River through the Grand Canyon occurred between ~5-6 Ma (e.g., Lucchitta, 1990; Dorsey et al., 2007). Given that incision along the western slope appears to initiate prior to this time – shortly after ~10 Ma along the Colorado River (Aslan et al., 2010; Karlstrom et al., 2012) and ~6-9 Ma along tributaries of the Green River (this study) – transient incision associated with the final integration of Grand Canyon is unlikely to be the primary driver for the initiation of incision in the Colorado Rockies. Rather, the data presented here bolster the interpretation that transient incision associated with integration of the Colorado River through Grand Canyon is restricted to the middle reaches of the Colorado River (Wolkowinsky and Granger, 2004; Karlstrom et al., 2008; Cook et al., 2009; Darling et al., 2012).

Our results do not preclude the possibility of an older drainage integration event upstream of Lee's Ferry, however. The presence of ~1500 meters of relief that developed between 35 Ma and 16 Ma in the southern Colorado Plateau (Flowers et al., 2007; Cather et al., 2008) suggest that a paleo-drainage divide may have existed somewhere to the south of the present day Book Cliffs (Lazear et al., 2013). It is possible that breaching of that divide led to incision along the upper Colorado River and Green River systems, but importantly, this hypothetical event must have pre-dated final integration of the Colorado River through Grand Canyon at ca. 5-6 Ma. Thus, although data from this study seem to rule out incision driven by drainage integration through Grand Canyon, they leave open the possibility that integration of the upper Colorado River was achieved through a protracted series of integration events.

Relatively little is known about the timing of breeching across the Book Cliffs and the integration of the Green River into the Colorado watershed. It has been hypothesized, however, that the Green River was relatively recently integrated into the Colorado watershed across the Uinta Mountains (Hansen, 1986). Recent dating of high terraces in the Green River basin, downstream of this point, suggest this event occurred before ~1.2 Ma (Darling et al., 2012) and sometime after ~8 Ma (Hansen, 1986). It seems probable that this integration event explains the ~100-200 m of relief across the knickzone along the Yampa River through Dinosaur Canyon (Figure 11E). However, the fact that this knickzone appears to be confined to the lower reaches of the river implies that it is not responsible for the incision we reconstruct along the western slope tributaries.

Importantly, given the modern drainage configuration, the hypothesis that differences in the amount of incision along the Colorado River (~1500 m) and the White/Yampa/Little Snake (~500-900 m) reflect a wave of incision that has propagated upstream along the Colorado River, but has not yet reached the northern tributaries (e.g., Pederson et al., 2013), requires that transient incision stalled across the knickzone along the Green River (Desolation and Grey Canyons,

Figure 9). There are two problems with this hypothesis. First, the drop in elevation along the Green River through these canyons is < 200 m, and thus there does not appear to be enough relief along the steepened reach of the profile to explain the observed difference in incision (~600-1000 m). The second problem with the hypothesis that incision was driven only by base level fall (Pederson et al., 2013, but cf., Karlstrom et al., 2013) is that it fails to explain nearly simultaneous incision in both the headwaters of the Colorado River as well as in the Little Snake River. As our results demonstrate, the best estimates of the onset of fluvial incision along both systems is between ~8-9 Ma, although it remains possible that much of the incision along the Yampa River took place post ~6 Ma. Thus, if incision across the western slope is entirely a response to drainage integration through Grand Canyon, it would require a scenario in which nearly instantaneous propagation of an initial wave of incision made its way throughout the entire system. For unknown reasons, this wave of incision would have continued along the Colorado River, but stalled along the Green River in Grey/Desolation canyons (Figure 9). As we argue below, we find it more likely that incision was driven by local changes in channel gradient during tilting across the western slope.

**Differential Rock Uplift and Tilting across the Western Slope**

As argued above, neither climatically enhanced incision nor basin integration seem sufficient to explain the patterns of fluvial incision and channel steepness along the western slope of the Colorado Rockies, which appears to leave open the possibility of differential rock uplift between the Colorado Rockies and the Colorado Plateau (e.g., Karlstrom et al., 2012; Darling et al., 2012). The association of steep channels in regions of large-magnitude incision is consistent with this hypothesis, as we expect such relationships in systems adjusted to spatial variations in rock uplift (e.g., Kirby et al., 2003). In the Colorado Rockies, moreover, the spatial correspondence between steep, rapidly incising rivers and presumably buoyant, low-seismic-velocity mantle (Karlstrom et al., 2012) suggests the possibility of a genetic association between fluvial incision and low-velocity mantle beneath the central Colorado Rockies.

At a regional scale, spatial differences in channel steepness, normalized for lithology (Figure 12), provides perhaps the strongest evidence for a tectonic component driving late Cenozoic incision. Without some forcing mechanism to drive channel steepening in the face of continuing incision, it is hard to explain why rivers would exhibit such systematic differences along the western slope. However, if low velocity mantle beneath Colorado is associated with dynamic support of topography, our data suggest that the flanks of the anomaly could be (or have been) characterized by long-wavelength tilting between the central Rockies and the Colorado Plateau. Notably, the width of regions of elevated steepness along rivers appears to correspond roughly with the degree to which channels extend across the region of low-velocity mantle (Figure 13). The Colorado River maintains a steep profile ($k_{sn}$ ~ 80-120 $m^{0.9}$) from Grand Junction to just below Gore Canyon (Figure 11), where it crosses the axis of low velocity mantle (Figure 13). In contrast, the White and Yampa Rivers only steepen in the upper ~100 km of their profiles (Figure 11), coincident with where they extend over the region of lowest seismic velocities (Figure 13), and the Little Snake River exhibits relatively uniform steepness values along its entire length, consistent with its position off the flank of the anomaly. We suggest that these associations indicate that channel profiles are still responding to a pulse of uplift that began within the last 6-9 Ma; this adjustment may still be ongoing, as suggested by the knickpoint along the Gunnison River (Donahue et al., 2013).

Some of the apparent tilting and differential rock uplift inferred from the pattern of incision could be a consequence of rebound related to unloading of the lithosphere (e.g., Wager, 1937; Molnar and England, 1990; Small and Anderson, 1995; Pederson et al., 2013). Most attempts to estimate the magnitude and distribution of isostatic rebound across the Colorado Plateau rely on volumetric reconstruction of material eroded over the past 10 – 30 Ma (Pederson et al., 2002; McMillan et al., 2006; Lazear et al., 2013) and yield generally similar patterns with a locus of rebound in the central and southern Colorado Plateau. The most recent of these models (Lazear et al., 2013) makes refined predictions for the amount of rebound along the western slope of the Rockies, which we rely on here as the current best estimate. In the vicinity of the Little Snake River, rebound is predicted to have been between 300 – 400 m (Figure 7 of Lazear et al., 2013), a value which could explain a sizable fraction of the 500 – 600 m of incision we observe. Predicted rebound increases toward the south, but remains between 500 – 700 m along most of the Colorado River upstream of Grand Junction (Figure 7 of Lazear et al., 2013). Thus, although isostatic rebound in response to late Cenozoic exhumation has the potential to explain some of the observed incision along rivers draining the western slope, it does not appear to be sufficient to explain the full signal.

Overall, the results of our study appear to require Late Cenozoic tilting along the western slope of the Colorado Rockies. Although a quantitative estimate remains beyond our ability to determine, it seems that patterns of incision require several hundred meters of differential rock uplift, in excess of isostatic adjustment, that range from ~200 m in northern Colorado to perhaps as much as ~700 m along the Colorado River. We note that these values are similar to the magnitude and wavelength observed along the eastern slope of the Rockies (e.g., McMillan et al., 2002; Leonard, 2002; Nereson et al., 2013), suggesting that both flanks of the range may be responding to changes in mantle buoyancy beneath central Colorado. We also note that the presence of Late Cenozoic alkalic volcanism in the Yampa region (Cosca et al., 2014; this study), extensional deformation (e.g., Buffler, 2003) are both consistent with the addition of buoyancy associated with continued modification of the mantle lithosphere beneath the range (e.g., Hansen et al., 2013). We suggest that long-wavelength tilting along the flanks of the range during the past 6 – 10 Ma has a tectonic origin associated with differences in the buoyancy of the mantle between the northern Rocky Mountains and adjacent regions.

## CONCLUSIONS

New chronology of basalt flows in the headwaters of the White, Yampa, and Little Snake Rivers allow estimates of the magnitude and timing of fluvial incision along the western slope of the Colorado Rockies. Combined with detailed analysis of the steepness of channel profiles ($k_{sn}$), these data provide new insights into the history and potential drivers of Late Cenozoic fluvial incision across the western slope of the Rocky Mountains and lead to the following conclusions:

1. Incision along the White, Yampa and Little Snake rivers post-dates ~9 - 10 Ma and most likely pre-dates 6 Ma. This is broadly synchronous with previous studies that infer post-8 – 10 Ma incision along the Colorado River.
2. Channel profile steepness ($k_{sn}$) of major river systems increase from north to south along the western slope, such that the Colorado River is two to three times as steep as the Little Snake River. These differences in profile steepness are independent of both discharge (e.g., Pederson and Tressler, 2012) and substrate lithology.
3. Spatial variations in channel steepness coincide with apparent differences in the magnitude of late Cenozoic incision. Incision along the Colorado River approaches ~1500 m, whereas incision along the White and Yampa river is less, ~700-900 m, and incision along the Little Snake is even lower, ~550 m.
4. Collectively, the association between steep channels, deep exhumation, and low velocity mantle at depth appears to implicate differential rock uplift during the past ~10 Ma as the best explanation for late Miocene – recent incision along the western slope of the Rockies.

**ACKNOWLEDGEMENTS**

This study was funded by the NSF- CREST project (Colorado Rockies Experiment and Seismic Transects) EAR-0607808. Additional support provided from EAR-0711546 (KEK) and EAR-1119635 (KEK and AA). Brandon Schmandt provided the EarthScope + CREST–derived tomographic images. We thank three anonymous reviewers and the Guest Associate Editor for comments that helped improve the manuscript.

## REFERENCES CITED


Anderson, R.S., Riihimaki, C.A., Safran, E.B., and MacGregor, K.R., 2006, Facing reality: Late Cenozoic evolution of smooth peaks, glacially ornamented valleys, and deep river gorges of Colorado's Front Range: Geological Society of America Special Papers, v. 398, p. 397–418, doi: 10.1130/2006.2398(25).

Aslan, A., Hood, W.C., Karlstrom, K.E., Kirby, E., Granger, D., Kelley, S.A., Crow, R., and Donahue, M.S., in press, Abandonment of Unaweep Canyon (1.4 to 0.8 Ma), western Colorado: effects of stream capture and anomalous rapid late Quaternary river incision: Geosphere, in press, MONTH???, 2014.

Aslan, A., Karlstrom, K.E., Crossey, L.J., Kelley, S., Cole, R., Lazear, G., and Darling, A., 2010, Late Cenozoic evolution of the Colorado Rockies: Evidence for Neogene uplift and drainage integration: Field Guides, v. 18, p. 21–54, doi: 10.1130/2010.0018(02).

Aslan, A., Karlstrom, K., Hood, W.C., Cole, R.D., Oesleby, T.W., Betton, C., Sandoval, M.M., Darling, A., Kelley, S., Hudson, A., Kaproth, B., Schoepfer, S., Benage, M., and Landman, R., 2008, River incision histories of the Black Canyon of the Gunnison and Unaweep Canyon: Interplay between late Cenozoic tectonism, climate change, and drainage integration in the western Rocky Mountains: Field Guides, v. 10, p. 175–202, doi: 10.1130/2008.fld010(09).

Aster, R., MacCarthy, J., Heizler, M., Kelley, S., Karlstrom, K., Crossey, L., and Dueker, K., 2009, CREST experiment probes the roots and geologic history of the Colorado Rockies: Outcrop, v. 58, no. 1, p. 6–23.

Berlin, M.M., 2009, Knickpoint Migration and Landscape Evolution on the Roan Plateau, Western Colorado [Ph.D. thesis]: Boulder, University of Colorado, 242 p.

Berlin, M.M., and Anderson, R.S., 2007, Modeling of knickpoint retreat on the Roan Plateau, western Colorado: Journal of Geophysical Research-Earth Surface, v. 112, no. F3, p. F03S06, doi: 10.1029/2006JF000553.

Bierman, P.R., and Steig, E.J., 1996, Estimating rates of denudation using cosmogenic isotope abundances: Earth Surface Processes and Landforms, v. 21, no. 2, p. 125–139.

Bookhagen, B., and Strecker, M.R., 2012, Spatiotemporal trends in erosion rates across a pronounced rainfall gradient: Examples from the southern Central Andes: Earth and Planetary Science Letters, v. 327–328, p. 97–110, doi: 10.1016/j.epsl.2012.02.005.

Borass, M., and Aslan, A., 2013, New detrital zircon ages and the paleogeography of Oligocene fluvial systems in the southern Green River Basin, Wyoming: Geological Society of America Abstracts with Programs, v. 45, no. 7, p. 563.

Bostick, N.H., and Freeman, V.L., 1984, Tests of vitrinite reflectance and paleotemperature models at the Multiwell Experiment site, Piceance Creek basin, Colorado: US Geological Survey Open-File Report 84-757, p. 110–120.

Buffler, R.T., 1967, The Browns Park Formation and its Relationship to the Late Tertiary Geologic History of the Elkhead Region [Ph.D. thesis]: Berkley, University of California, 175 p.

Buffler, R.T., 2003, The Browns Park Formation in the Elkhead Region, northwestern Colorado–south central Wyoming: Implications for late Cenozoic sedimentation, *in* Raynolds, R.G. and Flores, R.M. eds., Cenozoic Systems of the Rocky Mountain Region, Rocky Mountain Section (SEPM), Denver, Colorado, p. 183–212.

Burbank, D.W., and Anderson, R.S., 2011, Tectonic Geomorphology: West Sussex, Wiley-Blackwell, 480 p.

Cather, S.M., Connell, S.D., Chamberlin, R.M., McIntosh, W.C., Jones, G.E., Potochnik, A.R., Lucas, S.G., and Johnson, P.S., 2008, The Chuska erg: Paleogeomorphic and paleoclimatic implications of an Oligocene sand sea on the Colorado Plateau: Geological Society of America Bulletin, v. 120, no. 1-2, p. 13 –33, doi: 10.1130/B26081.1.

Coblentz, D., Chase, C.G., Karlstrom, K.E., and van Wijk, J., 2011, Topography, the geoid, and compensation mechanisms for the southern Rocky Mountains: Geochemistry, Geophysics, Geosystems, v. 12, no. 4, p. Q04002, doi: 10.1029/2010GC003459.

Cole, R.D., 2010, Eruptive history of the Grand Mesa Basalt Field, western Colorado: Geological Society of America Abstracts with Programs, v. 42, no. 5, p. 76.

Cook, K.L., Whipple, K.X., Heimsath, A.M., and Hanks, T.C., 2009, Rapid incision of the Colorado River in Glen Canyon – insights from channel profiles, local incision rates, and modeling of lithologic controls: Earth Surface Processes and Landforms, v. 34, no. 7, p. 994–1010, doi: 10.1002/esp.1790.

Cosca, M.A., Thompson, R.A., Lee, J.P., Turner, K.J., Neymark, L.A., and Premo, W.R., 2014, $^{40}$Ar/$^{39}$Ar geochronology, isotope geochemistry (Sr, Nd, Pb), and petrology of alkaline lavas near Yampa, Colorado: Migration of alkaline volcanism and evolution of the northern Rio Grande rift: Geosphere,, doi: 10.1130/GES00921.1.

Crosby, B.T., and Whipple, K.X., 2006, Knickpoint initiation and distribution within fluvial networks: 236 waterfalls in the Waipaoa River, North Island, New Zealand: The Hydrology and Geomorphology of Bedrock Rivers, v. 82, no. 1–2, p. 16–38, doi: 10.1016/j.geomorph.2005.08.023.

Cyr, A.J., Granger, D.E., Olivetti, V., and Molin, P., 2010, Quantifying rock uplift rates using channel steepness and cosmogenic nuclide–determined erosion rates: Examples from northern and southern Italy: Lithosphere, v. 2, no. 3, p. 188–198.

Darling, A.L., Karlstrom, K.E., Aslan, A., Cole, R., Betton, C., and Wan, E., 2009, Quaternary incision rates and drainage evolution of the Uncompahgre and Gunnison Rivers, western Colorado, as calibrated by the Lava Creek B ash: Rocky Mountain Geology, v. 44, no. 1, p. 71–83.

Darling, A.L., Karlstrom, K.E., Granger, D.E., Aslan, A., Kirby, E., Ouimet, W.B., Lazear, G.D., Coblentz, D.D., and Cole, R.D., 2012, New incision rates along the Colorado River system based on cosmogenic burial dating of terraces: Implications for regional controls on Quaternary incision: Geosphere, v. 8, no. 5, p. 1020–1041, doi: 10.1130/GES00724.1.

Dethier, D.P., 2001, Pleistocene incision rates in the western United States calibrated using Lava Creek B tephra: Geology, v. 29, no. 9, p. 783–786, doi: 10.1130/0091-7613(2001)029<0783:PIRITW>2.0.CO;2.

DiBiase, R.A., and Whipple, K.X., 2011, The influence of erosion thresholds and runoff variability on the relationships among topography, climate, and erosion rate: Journal of Geophysical Research-Earth Surface, v. 116, no. F4, p. F04036, doi: 10.1029/2011JF002095.

DiBiase, R.A., Whipple, K.X., Heimsath, A.M., and Ouimet, W.B., 2010, Landscape form and millennial erosion rates in the San Gabriel Mountains, CA: Earth and Planetary Science Letters, v. 289, no. 1–2, p. 134–144, doi: 10.1016/j.epsl.2009.10.036.

Donahue, M.S., Karlstrom, K.E., Aslan, A., Darling, A., Granger, D., Wan, E., Dickinson, R.G., and Kirby, E., 2013, Incision history of the Black Canyon of Gunnison, Colorado, over the past ~1 Ma inferred from dating of fluvial gravel deposits: Geosphere, v. 9, no. 4, p. 815–826, doi: 10.1130/GES00847.1.

Dorsey, R.J., Fluette, A., McDougall, K., Housen, B.A., Janecke, S.U., Axen, G.J., and Shirvell, C.R., 2007, Chronology of Miocene–Pliocene deposits at Split Mountain Gorge, Southern California: A record of regional tectonics and Colorado River evolution: Geology, v. 35, no. 1, p. 57–60, doi: 10.1130/G23139A.1.

Duller, R.A., Whittaker, A.C., Swinehart, J.B., Armitage, J.J., Sinclair, H.D., Bair, A., and Allen, P.A., 2012, Abrupt landscape change post–6 Ma on the central Great Plains, USA: Geology, v. 40, no. 10, p. 871–874, doi: 10.1130/G32919.1.

Duvall, A., Kirby, E., and Burbank, D., 2004, Tectonic and lithologic controls on bedrock channel profiles and processes in coastal California: Journal of Geophysical Research-Earth Surface, v. 109, no. F3, p. F03002, doi: 10.1029/2003JF000086.

Elkins-Tanton, L.T., 2005, Continental magmatism caused by lithospheric delamination: Geological Society of America Special Papers, v. 388, p. 449–461, doi: 10.1130/0-8137-2388-4.449.

Finnegan, N.J., Roe, G., Montgomery, D.R., and Hallet, B., 2005, Controls on the channel width of rivers: Implications for modeling fluvial incision of bedrock: Geology, v. 33, no. 3, p. 229–232, doi: 10.1130/G21171.1.

Flint, J.J., 1974, Stream gradient as a function of order, magnitude, and discharge: Water Resources Research, v. 10, no. 5, p. 969–973, doi: 10.1029/WR010i005p00969.

Flowers, R.M., and Farley, K.A., 2012, Apatite $^4$He/$^3$He and (U-Th)/He Evidence for an Ancient Grand Canyon: Science, v. 338, no. 6114, p. 1616–1619, doi: 10.1126/science.1229390.

Flowers, R.M., Shuster, D.L., Wernicke, B.P., and Farley, K.A., 2007, Radiation damage control on apatite (U-Th)/He dates from the Grand Canyon region, Colorado Plateau: Geology, v. 35, no. 5, p. 447–450, doi: 10.1130/G23471A.1.

Forte, A.M., Moucha, R., Simmons, N.A., Grand, S.P., and Mitrovica, J.X., 2010, Deep-mantle contributions to the surface dynamics of the North American continent: Tectonophysics, v. 481, no. 1–4, p. 3–15, doi: 10.1016/j.tecto.2009.06.010.

Grams, P.E., and Schmidt, J.C., 1999, Geomorphology of the Green River in the eastern Uinta Mountains, Dinosaur National Monument, Colorado and Utah, *in* Miller, A.J. and Gupta, A. eds., Varieties of Fluvial Form, Chichester, John Wiley & Sons Ltd, p. 81–111.

Grand, S.P., 1994, Mantle shear structure beneath the Americas and surrounding oceans: Journal of Geophysical Research-Solid Earth, v. 99, no. B6, p. 11591–11621, doi: 10.1029/94JB00042.

Granger, D.E., Kirchner, J.W., and Finkel, R., 1996, Spatially Averaged Long-Term Erosion Rates Measured from in Situ-Produced Cosmogenic Nuclides in Alluvial Sediment: The Journal of Geology, v. 104, no. 3, p. 249–257, doi: 10.2307/30068190.

Green, G.N., 1992, Digital Geologic Map of Colorado in ARC/INFO Format: U.S. Geological Survey Open-File Report 92-507, scale 1:500,000.

Green, G.N., and Drouillard, P.H., 1994, Digital Geologic Map of Wyoming in ARC/INFO Format: U.S. Geological Survey Open-File Report 94-0425, scale 1:500,000.

Gregory, K.M., and Chase, C.G., 1994, Tectonic and climatic significance of a late Eocene low-relief, high-level geomorphic surface, Colorado: Journal of Geophysical Research, v. 99, no. B10, p. 20141–20160, doi: 10.1029/94JB00132.

Hansen, W.R., 1986, Neogene Tectonics and Geomorphology of the Eastern Uinta Mountains in Utah, Colorado, and Wyoming: U.S. Geological Survey Professional Paper 1356, p. 1–78.

Hansen, W.R., 1987, The Black Canyon of the Gunnison, Colorado, *in* Bues, S. ed., Centenial Field Guide, Geological Society of America, Rocky Mountain Section, Boulder, Colorado, p. 321–324.

Hansen, S.M., Dueker, K.G., Stachnik, J.C., Aster, R.C., and Karlstrom, K.E., 2013, A rootless rockies—Support and lithospheric structure of the Colorado Rocky Mountains inferred from CREST and TA seismic data: Geochemistry, Geophysics, Geosystems, v. 14, no. 8, p. 2670–2695, doi: 10.1002/ggge.20143.

Harkins, N., Kirby, E., Heimsath, A., Robinson, R., and Reiser, U., 2007, Transient fluvial incision in the headwaters of the Yellow River, northeastern Tibet, China: Journal of Geophysical Research-Earth Surface, v. 112, no. F3, p. F03S04, doi: 10.1029/2006JF000570.

Haviv, I., Enzel, Y., Whipple, K.X., Zilberman, E., Matmon, A., Stone, J., and Fifield, K.L., 2010, Evolution of vertical knickpoints (waterfalls) with resistant caprock: Insights from numerical modeling: Journal of Geophysical Research-Earth Surface, v. 115, no. F3, p. F03028, doi: 10.1029/2008JF001187.

Hintze, L.F., 1980, Geologic Map of Utah: Utah Geological and Mineral Survey A-1, scale 1:500,000, 2 sheets.

Hintze, L.F., Willis, G.C., Laes, D.Y.M., Sprinkel, D.A., and Brown, K.D., 2000, Digital Geologic Map of Utah: Utah Geological Survey 179DM, scale 1:500,000.

Howard, A.D., 1994, A detachment-limited model of drainage basin evolution: Water Resources Research, v. 30, no. 7, p. 2261–2285, doi: 10.1029/94WR00757.

Humphreys, E., Hessler, E., Dueker, K., Farmer, G.L., Erslev, E., and Atwater, T., 2003, How Laramide-age hydration of North American lithosphere by the Farallon slab controlled subsequent activity in the western United States: International Geology Review, v. 45, no. 7, p. 575–595.

Hunt, C.B., 1956, Cenozoic geology of the Colorado Plateau: U.S. Geological Survey Professional Paper 279, p. 1-97.

Izett, G.A., 1975, Late Cenozoic Sedimentation and deformation in northern Colorado and adjoining areas, *in* Curtis, B.F. ed., Cenozoic history of the south Rocky Mountains: Geological Society of America Memoir 144, p. 179–207.

Izett, G.A., Denson, N.M., and Obradovich, J.D., 1970, K-Ar age of the lower part of the Browns Park Formation, northwestern Colorado: U.S. Geological Survey Professional Paper 700-C, p. C150–C152.

Karlstrom, K.E., Coblentz, D., Dueker, K., Ouimet, W., Kirby, E., Van Wijk, J., Schmandt, B., Kelley, S., Lazear, G., Crossey, L.J., Crow, R., Aslan, A., Darling, A., Aster, R., MacCarthy, J., Hansen, S.M., Stachnik, J., Stockli, D.F., Garcia, R.V., Hoffman, M., McKeon, R., Feldman, J., Heizler, M., Donahue, M.S., and the CREST Working Group, 2012, Mantle-driven dynamic uplift of the Rocky Mountains and Colorado Plateau and its surface response: Toward a unified hypothesis: Lithosphere, v. 4, no. 1, p. 3 –22, doi: 10.1130/L150.1.

Karlstrom, K.E., Crow, R., Crossey, L.J., Coblentz, D., and Van Wijk, J.W., 2008, Model for tectonically driven incision of the younger than 6 Ma Grand Canyon: Geology, v. 36, no. 11, p. 835 –838, doi: 10.1130/G25032A.1.

Karlstrom, K.E., Lee, J.P., Kelley, S.A., Crow, R.S., Crossey, L.J., Young, R.A., Lazear, G., Beard, L.S., Ricketts, J.W., Fox, M., and Shuster, D.L., 2014, Formation of the Grand Canyon 5 to 6 million years ago through integration of older palaeocanyons: Nature Geoscience, v. 7, no. 3, p. 239–244.

Karlstrom, K.E., Darling, A., Crow, R., Lazear, G., Aslan, A., Granger, D., Kirby, E., Crossey, L., and Whipple, K., 2013, Colorado River chronostratigraphy at Lee's Ferry, Arizona, and the Colorado Plateau bull's eye of incision; Forum Comment: Geology, doi:10.1130/G34550C.1.

Kirby, E., Johnson, C., Furlong, K., and Heimsath, A., 2007, Transient channel incision along Bolinas Ridge, California: Evidence for differential rock uplift adjacent to the San Andreas fault: Journal of Geophysical Research-Earth Surface, v. 112, no. F3, p. F03S07, doi: 10.1029/2006JF000559.

Kirby, E., and Ouimet, W., 2011, Tectonic geomorphology along the eastern margin of Tibet: insights into the pattern and processes of active deformation adjacent to the Sichuan Basin: Geological Society, London, Special Publications, v. 353, no. 1, p. 165–188, doi: 10.1144/SP353.9.

Kirby, E., and Whipple, K.X., 2012, Expression of active tectonics in erosional landscapes: Journal of Structural Geology, v. 44, p. 54–75, doi: 10.1016/j.jsg.2012.07.009.

Kirby, E., and Whipple, K., 2001, Quantifying differential rock-uplift rates via stream profile analysis: Geology, v. 29, no. 5, p. 415–418, doi: 10.1130/0091-7613(2001)029<0415:QDRURV>2.0.CO;2.

Kirby, E., Whipple, K.X., Tang, W., and Chen, Z., 2003, Distribution of active rock uplift along the eastern margin of the Tibetan Plateau: Inferences from bedrock channel longitudinal profiles: Journal of Geophysical Research-Solid Earth, v. 108, no. B4, p. ETG 16, doi: 10.1029/2001JB000861.

Kucera, R.E., 1962, Geology of the Yampa District, Northwest Colorado [Ph.D. dissertation]: Boulder, University of Colorado, 675 p.

Kuhlemann, J., Frisch, W., Székely, B., Dunkl, I., and Kázmér, M., 2002, Post-collisional sediment budget history of the Alps: tectonic versus climatic control: International Journal of Earth Sciences, v. 91, no. 5, p. 818–837.

Kunk, M.J., Budahn, J.R., Unruh, D.M., Stanley, J.O., Kirkham, R.M., Bryant, B., Scott, R.B., Lidke, D.J., and Streufert, R.K., 2002, $^{40}$Ar/$^{39}$Ar ages of late Cenozoic volcanic rocks within and around the Carbondale and Eagle collapse centers, Colorado: Constraints on the timing of evaporite-related collapse, *in* Scott, R.B., Kirkham, R.M., and Judkins, T.W. eds., Late Cenozoic evaporite tectonism and volcanism in west-central Colorado: Geological Society of America Special Paper 366, p. 15–30.

Lague, D., Hovius, N., and Davy, P., 2005, Discharge, discharge variability, and the bedrock channel profile: Journal of Geophysical Research-Earth Surface, v. 110, no. F4, p. F04006, doi: 10.1029/2004JF000259.

Lanphere, M.A., Champion, D.E., Christiansen, R.L., Izett, G.A., and Obradovich, J.D., 2002, Revised ages for tuffs of the Yellowstone Plateau volcanic field: Assignment of the Huckleberry Ridge Tuff to a new geomagnetic polarity event: Geological Society of America Bulletin, v. 114, no. 5, p. 559 –568, doi: 10.1130/0016-7606(2002)114<0559:RAFTOT>2.0.CO;2.

Larson, E.E., Ozima, M., and Bradley, W.C., 1975, Late Cenozoic Basic Volcanism in Northwestern Colorado and Its Implications Concerning Tectonism and the Origin of the

Colorado River System, *in* Curtis, B.F. ed., Cenozoic history of the south Rocky Mountains: Geological Society of America Memoir 144, p. 155–178.

Lazear, G., Karlstrom, K., Aslan, A., and Kelley, S., 2013, Denudation and flexural isostatic response of the Colorado Plateau and southern Rocky Mountains region since 10 Ma: Geosphere, v. 9, no. 4, p. 1-23, doi: 10.1130/GES00836.1.

Leonard, E.M., 2002, Geomorphic and tectonic forcing of late Cenozoic warping of the Colorado piedmont: Geology, v. 30, no. 7, p. 595–598.

Levander, A., Schmandt, B., Miller, M.S., Liu, K., Karlstrom, K.E., Crow, R.S., Lee, C.-T.A., and Humphreys, E.D., 2011, Continuing Colorado plateau uplift by delamination-style convective lithospheric downwelling: Nature, v. 472, no. 7344, p. 461–465, doi: 10.1038/nature10001.

Liu, L., and Gurnis, M., 2010, Dynamic subsidence and uplift of the Colorado Plateau: Geology, v. 38, no. 7, p. 663–666, doi: 10.1130/G30624.1.

Love, J.D., and Christiansen, A.C., 1985, Geologic Map of Wyoming: U.S. Geological Survey, scale 1:500,000, 3 sheets.

Lucchitta, I., 1990, History of the Grand Canyon and the Colorado River in Arizona, *in* Bues, S. and Morales, M. eds., Grand Canyon Geology, New York, Oxford University Press, p. 311–332.

Luft, S.J., 1985, Airfall tuff in the Browns Park Formation, northwestern Colorado and northeastern Utah: The Mountain Geologist, v. 22, no. 3, p. 110–127.

Mackin, J.H., 1948, Concept of the graded river: Geological Society of America Bulletin, v. 59, no. 5, p. 463–512.

McMillan, M.E., Angevine, C.L., and Heller, P.L., 2002, Postdepositional tilt of the Miocene-Pliocene Ogallala Group on the western Great Plains: Evidence of late Cenozoic uplift of the Rocky Mountains: Geology, v. 30, no. 1, p. 63 –66, doi: 10.1130/0091-7613(2002)030<0063:PTOTMP>2.0.CO;2.

McMillan, M.E., Heller, P.L., and Wing, S.L., 2006, History and causes of post-Laramide relief in the Rocky Mountain orogenic plateau: Geological Society of America Bulletin, v. 118, no. 3-4, p. 393 –405, doi: 10.1130/B25712.1.

Merritts, D., and Vincent, K.R., 1989, Geomorphic response of coastal streams to low, intermediate, and high rates of uplift, Medocino triple junction region, northern California: Geological Society of America Bulletin, v. 101, no. 11, p. 1373–1388.

Moglen, G.E., and Bras, R.L., 1995, The importance of spatially heterogeneous erosivity and the cumulative area distribution within a basin evolution model: Geomorphology, v. 12, no. 3, p. 173–185, doi: 10.1016/0169-555X(95)00003-N.

Molnar, P., 2001, Climate change, flooding in arid environments, and erosion rates: Geology, v. 29, no. 12, p. 1071–1074, doi: 10.1130/0091-7613(2001)029<1071:CCFIAE>2.0.CO;2.

Molnar, P., 2004, Late Cenozoic Increase In Accumulation Rates Of Terrestrial Sediment: How Might Climate Change Have Affected Erosion Rates?: Annual review of earth and planetary sciences, v. 32, no. 1, p. 67–89, doi: 10.1146/annurev.earth.32.091003.143456.

Molnar, P., and England, P., 1990, Late Cenozoic uplift of mountain ranges and global climate change: chicken or egg?: Nature, v. 346, no. 6279, p. 29–34, doi: 10.1038/346029a0.

Morell, K.D., Kirby, E., Fisher, D.M., and van Soest, M., 2012, Geomorphic and exhumational response of the Central American Volcanic Arc to Cocos Ridge subduction: Journal of Geophysical Research-Solid Earth, v. 117, no. B4, p. B04409, doi: 10.1029/2011JB008969.

Moucha, R., Forte, A.M., Rowley, D.B., Mitrovica, J.X., Simmons, N.A., and Grand, S.P., 2008, Mantle convection and the recent evolution of the Colorado Plateau and the Rio Grande Rift valley: Geology, v. 36, no. 6, p. 439–442, doi: 10.1130/G24577A.1.

Naeser, C.W., Izett, G.A., and Obradovich, J.D., 1980, Fission-track and K-Ar ages of natural glasses: Geological Survey Bulletin 1489, p. 1–31.

Nereson, A., Stroud, J., Karlstrom, K., Heizler, M., and McIntosh, W., 2013, Dynamic topography of the western Great Plains: Geomorphic and $^{40}$Ar/$^{39}$Ar evidence for mantle-driven uplift associated with the Jemez lineament of NE New Mexico and SE Colorado: Geosphere, v. 9, no. 3, p. 521–545, doi: 10.1130/GES00837.1.

Olivetti, V., Cyr, A.J., Molin, P., Faccenna, C., and Granger, D.E., 2012, Uplift history of the Sila Massif, southern Italy, deciphered from cosmogenic $^{10}$Be erosion rates and river longitudinal profile analysis: Tectonics, v. 31, no. 3, p. TC3007, doi: 10.1029/2011TC003037.

Ouimet, W.B., Whipple, K.X., and Granger, D.E., 2009, Beyond threshold hillslopes: Channel adjustment to base-level fall in tectonically active mountain ranges: Geology, v. 37, no. 7, p. 579–582, doi: 10.1130/G30013A.1.

Pederson, J.L., Cragun, W.S., Hidy, A.J., Rittenour, T.M., and Gosse, J.C., 2013, Colorado River chronostratigraphy at Lee's Ferry, Arizona, and the Colorado Plateau bull's-eye of incision: Geology, v. 41, no. 4, p. 427–430, doi: 10.1130/G34051.1.

Pederson, J.L., Mackley, R.D., and Eddleman, J.L., 2002, Colorado Plateau uplift and erosion evaluated using GIS: GSA Today, v. 12, no. 8, p. 4–10.

Pederson, J.L., and Tressler, C., 2012, Colorado River long-profile metrics, knickzones and their meaning: Earth and Planetary Science Letters, v. 345–348, p. 171–179, doi: 10.1016/j.epsl.2012.06.047.

Pelletier, J., 2009, The impact of snowmelt on the late Cenozoic landscape of the southern Rocky Mountains, USA: GSA Today, v. 19, no. 7, p. 4–10, doi: 10.1130/GSATG44A.1.

Perron, J.T., and Royden, L., 2013, An integral approach to bedrock river profile analysis: Earth Surface Processes and Landforms, v. 38, no. 6, p. 570–576, doi: 10.1002/esp.3302.

Powell, J.W., 1876, Report on the geology of the eastern portion of the Uinta Mountains and a region of country adjacent thereto: Washington, D.C., U.S. Geologic and Geographic Survey.

Reiter, M., 2008, Geothermal anomalies in the crust and upper mantle along Southern Rocky Mountain transitions: Geological Society of America bulletin, v. 120, no. 3-4, p. 431–441, doi: 10.1130/B26198.1.

Riihimaki, C.A., Anderson, R.S., and Safran, E.B., 2007, Impact of rock uplift on rates of late Cenozoic Rocky Mountain river incision: Journal of Geophysical Research-Earth Surface, v. 112, no. F3, p. F03S02, doi: 10.1029/2006JF000557.

Roe, G.H., Montgomery, D.R., and Hallet, B., 2002, Effects of orographic precipitation variations on the concavity of steady-state river profiles: Geology, v. 30, no. 2, p. 143–146, doi: 10.1130/0091-7613(2002)030<0143:EOOPVO>2.0.CO;2.

Roy, M., Jordan, T.H., and Pederson, J., 2009, Colorado Plateau magmatism and uplift by warming of heterogeneous lithosphere: Nature, v. 459, no. 7249, p. 978–982, doi: 10.1038/nature08052.

Roy, M., Kelley, S., Pazzaglia, F., Cather, S., and House, M., 2004, Middle Tertiary buoyancy modification and its relationship to rock exhumation, cooling, and subsequent extension at the eastern margin of the Colorado Plateau: Geology, v. 32, no. 10, p. 925–928, doi: 10.1130/G20561.1.

Royden, L., and Perron, J.T., 2013, Solutions of the stream power equation and application to the evolution of river longitudinal profiles: Journal of Geophysical Research-Earth Surface, v. 118, no. 2, p. 497–518, doi: 10.1002/jgrf.20031.

Safran, E.B., Bierman, P.R., Aalto, R., Dunne, T., Whipple, K.X., and Caffee, M., 2005, Erosion rates driven by channel network incision in the Bolivian Andes: Earth Surface Processes and Landforms, v. 30, no. 8, p. 1007–1024, doi: 10.1002/esp.1259.

Sandoval, M.M., 2007, Quaternary Incision History of the Black Canyon of the Gunnison, Colorado [M.S. thesis]: Albuquerque, University of New Mexico, 96 p.

Sass, J.H., Lachenbruch, A.H., Munroe, R.J., Greene, G.W., and Moses, T.H., 1971, Heat flow in the western United States: Journal of Geophysical Research, v. 76, no. 26, p. 6376–6413, doi: 10.1029/JB076i026p06376.

Schmandt, B., and Humphreys, E., 2010, Complex subduction and small-scale convection revealed by body-wave tomography of the western United States upper mantle: Earth and Planetary Science Letters, v. 297, no. 3–4, p. 435–445, doi: 10.1016/j.epsl.2010.06.047.

Seeber, L., and Gornitz, V., 1983, River profiles along the Himalayan arc as indicators of active tectonics: Tectonophysics, v. 92, no. 4, p. 335–367, doi: 10.1016/0040-1951(83)90201-9.

Sheehan, A.F., Abets, G.A., Jones, C.H., and Lerner-Lam, A.L., 1995, Crustal thickness variations across the Colorado Rocky: Journal of Geophysical Research, v. 100, no. B10, p. 391–404.

Sklar, L., and Dietrich, W.E., 1998, River Longitudinal Profiles and Bedrock Incision Models: Stream Power and the Influence of Sediment Supply, *in* Tinkler, J. and Wohl, E. eds., Rivers Over Rock: Fluvial Processes in Bedrock Channels, Geophysical Monograph Series, Washington, D.C., American Geophysical Union, p. 237–260.

Small, E.E., and Anderson, R.S., 1995, Geomorphically Driven Late Cenozoic Rock Uplift in the Sierra Nevada, California: Science, v. 270, no. 5234, p. 277–281, doi: 10.1126/science.270.5234.277.

Snyder, G.L., 1980, Geologic map of the northernmost Park Range and the southernmost Sierra Madre, Jackson and Routt Counties, Colorado: U.S. Geological Survey Misc. Investigations Map I-1113, scale 1:48,000, 1 sheet.

Snyder, N.P., Whipple, K.X., Tucker, G.E., and Merritts, D.J., 2003, Importance of a stochastic distribution of floods and erosion thresholds in the bedrock river incision problem: Journal of Geophysical Research-Solid Earth, v. 108, no. B2, p. 2117, doi: 10.1029/2001JB001655.

Snyder, N.P., Whipple, K.X., Tucker, G.E., and Merritts, D.J., 2000, Landscape response to tectonic forcing: Digital elevation model analysis of stream profiles in the Mendocino triple junction region, northern California: Geological Society of America Bulletin, v. 112, no. 8, p. 1250–1263, doi: 10.1130/0016-7606(2000)112<1250:LRTTFD>2.0.CO;2.

Tressler, C., 2011, From Hillslopes to Canyons, Studies of Erosion at Differing Time and Spatial Scales Within the Colorado River Drainage [M.S. thesis]: Logan, Utah State University, 99 p.

Tucker, G.E., 2004, Drainage basin sensitivity to tectonic and climatic forcing: implications of a stochastic model for the role of entrainment and erosion thresholds: Earth Surface Processes and Landforms, v. 29, no. 2, p. 185–205, doi: 10.1002/esp.1020.

Tweto, O., 1979, Geologic Map of Colorado: U.S. Geological Survey, scale 1:500,000, 2 sheets.

Tweto, O., 1976, Geologic Map of the Craig 1°x2° Quadrangle, Northwestern Colorado: U.S. Geological Survey Geological Survey Miscellaneous Investigations Series Map I-972, scale 1:250,000, 1 sheet.

Wager, L., 1937, The Arun River drainage pattern and the rise of the Himalaya: The Geographical journal, v. 89, no. 3, p. 239.

Wernicke, B., 2011, The California River and its role in carving Grand Canyon: Geological Society of America Bulletin, v. 123, no. 7-8, p. 1288–1316, doi: 10.1130/B30274.1.

Whipple, K.X., 2004, Bedrock rivers and the geomorphology of active orogens: Annual Review of Earth and Planetary Sciences, v. 32, no. 1, p. 151–185, doi: 10.1146/annurev.earth.32.101802.120356.

Whipple, K., DiBiase, R., and Crosby, B., 2012, Bedrock Rivers, *in* Owen, L. ed., Treatise in Fluvial Geomorphology.

Whipple, K.X., and Tucker, G.E., 1999, Dynamics of the stream-power river incision model: Implications for height limits of mountain ranges, landscape response timescales, and research needs: Journal of Geophysical Research: Solid Earth, v. 104, no. B8, p. 17661–17674, doi: 10.1029/1999JB900120.

Whipple, K.X., and Tucker, G.E., 2002, Implications of sediment-flux-dependent river incision models for landscape evolution: Journal of Geophysical Research-Solid Earth, v. 107, no. B2, p. ETG 3–1, doi: 10.1029/2000JB000044.

Whittaker, A.C., Attal, M., Cowie, P.A., Tucker, G.E., and Roberts, G., 2008, Decoding temporal and spatial patterns of fault uplift using transient river long profiles: Geomorphology, v. 100, no. 3–4, p. 506–526, doi: 10.1016/j.geomorph.2008.01.018.

Whittaker, A.C., Cowie, P.A., Attal, M., Tucker, G.E., and Roberts, G.P., 2007, Bedrock channel adjustment to tectonic forcing: Implications for predicting river incision rates: Geology, v. 35, no. 2, p. 103–106, doi: 10.1130/G23106A.1.

Van Wijk, J.W., Baldridge, W.S., van Hunen, J., Goes, S., Aster, R., Coblentz, D.D., Grand, S.P., and Ni, J., 2010, Small-scale convection at the edge of the Colorado Plateau: Implications for topography, magmatism, and evolution of Proterozoic lithosphere: Geology, v. 38, no. 7, p. 611–614, doi: 10.1130/G31031.1.

Willenbring, J.K., and von Blanckenburg, F., 2010, Long-term stability of global erosion rates and weathering during late-Cenozoic cooling: Nature, v. 465, no. 7295, p. 211–214, doi: 10.1038/nature09044.

Wobus, C.W., Kean, J.W., Tucker, G.E., and Anderson, R.S., 2008, Modeling the evolution of channel shape: Balancing computational efficiency with hydraulic fidelity: Journal of Geophysical Research-Earth Surface, v. 113, no. F2, p. F02004, doi: 10.1029/2007JF000914.

Wobus, C.W., Tucker, G.E., and Anderson, R.S., 2010, Does climate change create distinctive patterns of landscape incision?: Journal of Geophysical Research-Earth Surface, v. 115, no. F4, p. F04008, doi: 10.1029/2009JF001562.

Wobus, C., Whipple, K.X., Kirby, E., Snyder, N., Johnson, J., Spyropolou, K., Crosby, B., and Sheehan, D., 2006, Tectonics from topography: Procedures, promise, and pitfalls: Geological Society of America Special Papers, v. 398, p. 55–74, doi: 10.1130/2006.2398(04).

Wolkowinsky, A.J., and Granger, D.E., 2004, Early Pleistocene incision of the San Juan River, Utah, dated with $^{26}$Al and $^{10}$Be: Geology, v. 32, no. 9, p. 749–752, doi: 10.1130/G20541.1.

Zhang, P., Molnar, P., and Downs, W.R., 2001, Increased sedimentation rates and grain sizes 2-4 Myr ago due to the influence of climate change on erosion rates: Nature, v. 410, no. 6831, p. 891–897, doi: 10.1038/35073504.

**FIGURE CAPTIONS**

**Figure 1**: Topography, physiographic provinces, and major rivers of the western United States. Physiographic provinces shown by white dashed lines. Large black inset shows the study area and smaller insets outline the areas of Figure 3 and Figure 4.

**Figure 2**: Modern topography of the Rocky Mountain physiographic province and approximate extent of Tertiary basins (left panel) and differential P-wave velocity at 100 km depth (right panel). Isolines on the right panel correspond to 0.5% of differential P-wave velocity. Geographic points for reference: GJ -- Grand Junction, CO; R -- Rifle, CO; SB -- Steamboat Springs; CO, NP -- North Park, SP -- South Park; GM -- Grand Mesa; BC -- Book Cliffs; FT -- Flat Tops; SWB -- Sand Wash Basin; UB -- Unita Basin; PB -- Piceance Basin. Tomographic data from Schmandt and Humphreys (2010).

**Figure 3**: Simplified geologic map showing locations of previously dated markers which provide constraints on the timing and magnitude of incision along the Colorado River (modified from Green, 1992; Tweto, 1979). The location of evaporite collapse centers along the Colorado River (from Kunk et al., 2002) are also shown in white. Data for previously published incision markers along the Colorado River are given in Table 1.

**Figure 4**: Simplified geologic map showing the extent of the Browns Park Formation (modified from Green, 1992; Tweto, 1979; Green and Drouillard, 1994; Love and Christiansen, 1985; Hintze et al., 2000; Hintze, 1980). The extent of detailed study areas for this work (Figure 6: Elkhead Mountains, Figure 7: Flat Tops, Figure 8: Yampa River Valley) are shown above by white boxes. Localities constraining the age of the Browns Park Formation: 1, Dead Mexican Park (24.8 +/- 2.4 Ma --Snyder, 1980); 2, west bank of Little Snake River (24.8 +/- 0.8 Ma -- Izett et al., 1970); 3, City Mountain (7.6 +/- 0.4 Ma -- Buffler, 1967); 4, Vermillion Creek (7.2 +/- 0.6 Ma -- Naeser et al., 1980).

**Figure 5**: Field relationships between basalt flows, the Browns Park Formation, and the Little Snake River at Battle Mountain, WY in the Elkhead Mountains (photo: Russell Rosenberg). Basalt flows capping the Browns Park Formation provide an estimate of local relief generated during late Cenozoic incision.

**Figure 6**: Simplified geologic map of the Elkhead Mountains (modified from Green, 1992; Tweto, 1979; Green and Drouillard, 1994; Love and Christiansen, 1985). References for ages: 1 this study; 2 Snyder, 1980.

**Figure 7**: Simplified geologic map of the Flat Tops (modified from Green, 1992; Tweto, 1979). References for ages: 1 Kunk et al., 2002; 2 Larson et al., 1975. *Sugar Loaf Mountain ages range from 13.45 +/-0.16 Ma to 15.57 +/- 0.09 Ma (Kunk et al., 2002). Quaternary deposits are largely coarse debris and landslides.

**Figure 8**: Simplified geologic map of the Yampa River Valley (modified from Green, 1992; Tweto, 1979). Crowner deposits bound by dashed contact. References for ages: 1 this study; 2 Izett, 1975.

**Figure 9**: New and previously published constraints on the magnitude of incision (meters) and age constraints (Ma) along the western flank of the Colorado Rocky Mountains within the last 6 -

12 Ma. References as follows (superscript numbers also correspond to information provided in Table 1 and Table 2): [1,2,3,4,5,6,7,8,16] this study; [9,10] Larson et al., 1975; this study; [11,12,13] Kunk et al., 2002; [14,15] Berlin 2009; [17] Kunk et al., 2002; Aslan et al., 2010; Cole, 2010.

**Figure 13**: (A) Channel steepness ($k_{sn}$) determined along 10 km channel segments shown as colored lines, with study rivers highlighted in black. Excluded segments shown in green (see text for details): BC – Black Canyon of the Gunnison, D – Dinosaur Canyon, GW – Glenwood Canyon, G – Gore Canyon, P – Park Range, W – Westwater Canyon. (B) Interpolated channel steepness ($k_{sn}$) with white contours showing P-wave velocity at depth (see Figure 2). Tomographic data from Schmandt and Humphreys (2010).

**Figure 10**: Simplified geologic map showing major bedrock lithologies within the study area (modified from Green, 1992; Tweto, 1979; Green and Drouillard, 1994; Love and Christiansen, 1985; Hintze et al., 2000; Hintze, 1980). Major rivers labeled (north to south): LS -- Little Snake River, Y -- Yampa River, W -- White River, Gr -- Green River, C -- Colorado River, Gn -- Gunnison River, D -- Dolores River.

**Figure 11**: Longitudinal profiles of study rivers with 10 km spaced bins of normalized channel steepness and color coded mapped bedrock geology. Error bars show one standard deviation of local $k_{sn}$.

**Figure 12**: Comparison of average normalized channel steepness ($k_{sn}$) within identified lithologies (left y-axis) and the magnitude of incision (right y-axis) along the western slope. Lithologies are grouped into Tertiary sandstones and shales. Blue boxes correspond to the ~range of incision values observed for each river. Grey shading indicates the overall trend of normalized channel steepness values. Reaches excluded from channel steepness averages include (see text for details): 1) headwater reaches along the White and Yampa Rivers where the valley bottom is covered by coarse Quaternary debris (shown on Figure 7), 2) a short reach immediately downstream of pre-Cambrian rocks along the Little Snake (Figure 11D), and 3) the Yampa River through Dinosaur Canyon (Figure 11E).

## APPENDIX 1. $^{40}Ar/^{39}Ar$ ANALYTICAL METHODS AND RESUTLS

The $^{39}Ar/^{40}Ar$ age determinations for this study were provided by Matt Heizler at New Mexico Tech University. The following detailed description of methods and analytical techniques used were also provide by Matt Heizler and are a modified excerpt from the New Mexico Geochronology Research Laboratory internal report #: NMGRL-IR-771:

Groundmass concentrates were prepared from basaltic samples by choosing fragments visibly free of phenocrysts whereas biotite or sanidine was obtained by standard mineral separation procedures. The prepared samples were irradiated in three batches; either for 10 hours or for one hour at the USGS TRIGA reactor in Denver, CO along with the standard Fish Canyon tuff sanidine as a neutron flux monitor. Most samples were analyzed by the step-heating method using a defocused $CO_2$ laser to heat the samples (Tables A-1 – A-4). The age of the Sand Mountain Sample was determined by probability distribution of individual sanidine grain total fusion ages (Figure A-5). A summary of the preferred eruption ages along with a listing of the analytical methods is provided in Table A-1 and Table A-2 and the general operational details for the NMGRL can be found at internet site [http://geoinfo.nmt.edu/publications/openfile/argon/home/html](http://geoinfo.nmt.edu/publications/openfile/argon/home/html).

The sample age spectra are defined by 8 to 12 heating steps and each sample provides either a plateau or isochron age that range between ~4.6 and 12.6 Ma (Tables A-1 – A-4; Figures. A-1 – A-4). Groundmass samples typically record age spectra (Figures A-1 and A-2) with an initial non-radiogenic step that is often discordant (younger and older) from the remaining steps that are themselves somewhat scattered. Isochron analysis demonstrates that for many age spectra the discordance is explained by trapped excess $^{40}Ar$ (Figures A-3 and A-4). The preferred age for each sample is given by the method (weighted mean or isochron) that in most cases yielded the lowest MSWD for the chosen steps and contained the great part of the spectrum. This is summarized in Table A-1 and Table A-2 and labeled either plateau or isochron on each age spectrum (Figures A-1 and A-2). Regression values for the isochrones are given by the York (1969) method. The biotite spectra are overall flat, however isochron data suggest minor excess argon contamination and therefore the isochron age is chosen as the preferred age.

For most age spectrum analyses the majority of gas released yields well-defined plateau and/or isochron results and therefore the preferred ages are confidently assigned as eruption ages.

**References for Appendix 1**

Renne, P.R., Swisher, C.C., Deino, A.L., Karner, D.B., Owens, T.L., and DePaolo, D.J., 1998, Intercalibration of standards, absolute ages and uncertainties in $^{40}Ar/^{39}Ar$ dating: Chemical Geology, v. 145, no. 1–2, p. 117–152, doi: 10.1016/S0009-2541(97)00159-9.

Steiger, R., and Jäger, E., 1977, Subcommission on geochronology: convention on the use of decay constants in geo-and cosmochronology: Earth and Planetary Science Letters, v. 36, no. 3, p. 359–362.

Taylor, J.R., 1997, An introduction to error analysis: the study of uncertainties in physical measurements: Sausalito, University Science Books, 327 p.

York, D., 1968, Least squares fitting of a straight line with correlated errors: Earth and Planetary Science Letters, v. 5, p. 320–324, doi: 10.1016/S0012-821X(68)80059-7.

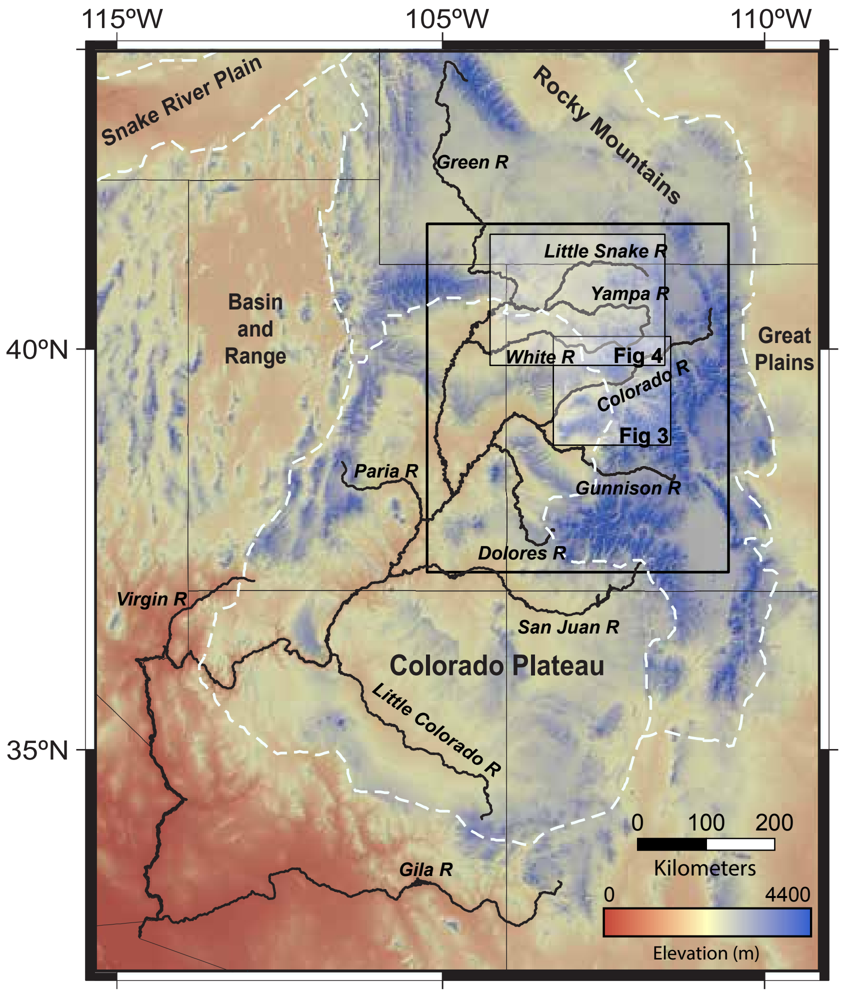


**Rosenberg et al., Figure 1**

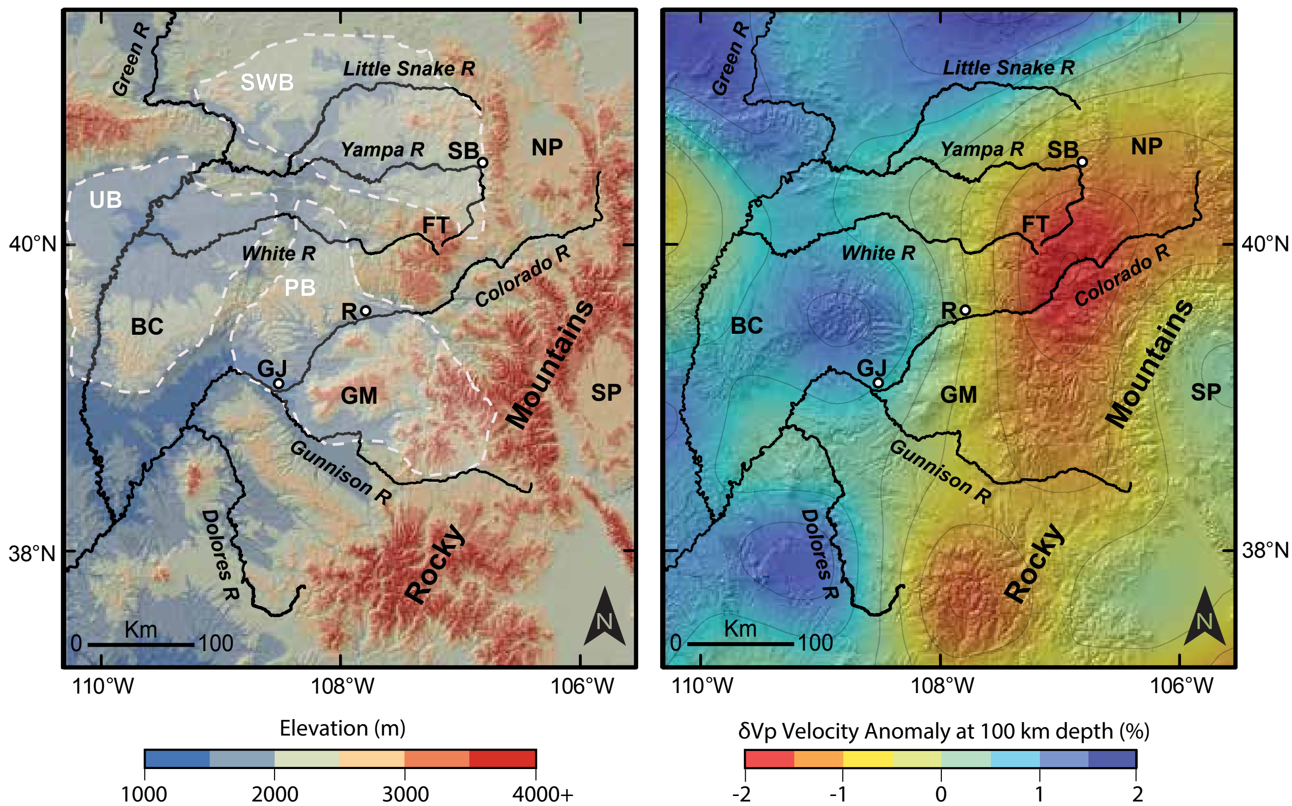


**Rosenberg et al., Figure 2**

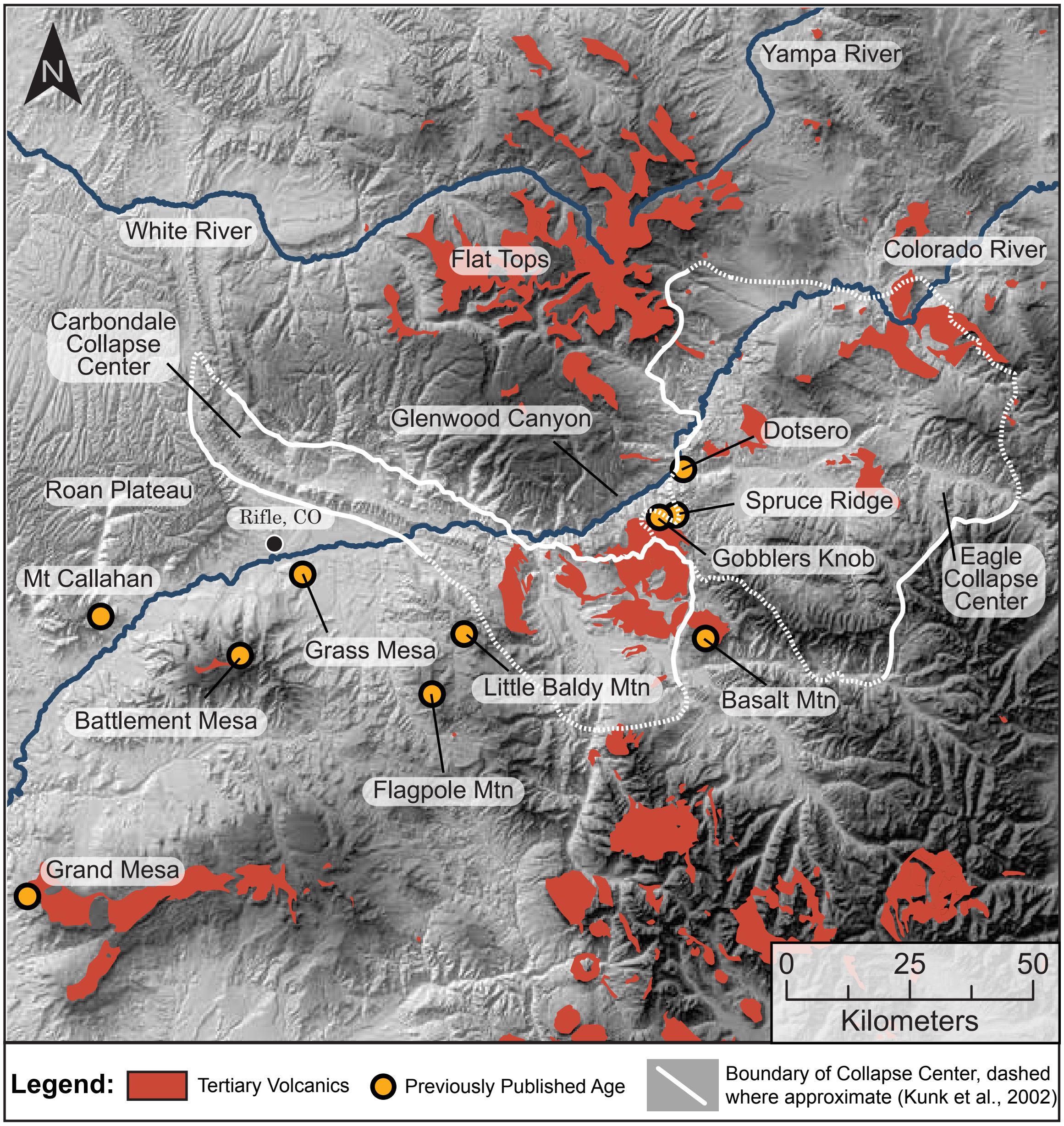


**Rosenberg et al., Figure 3**

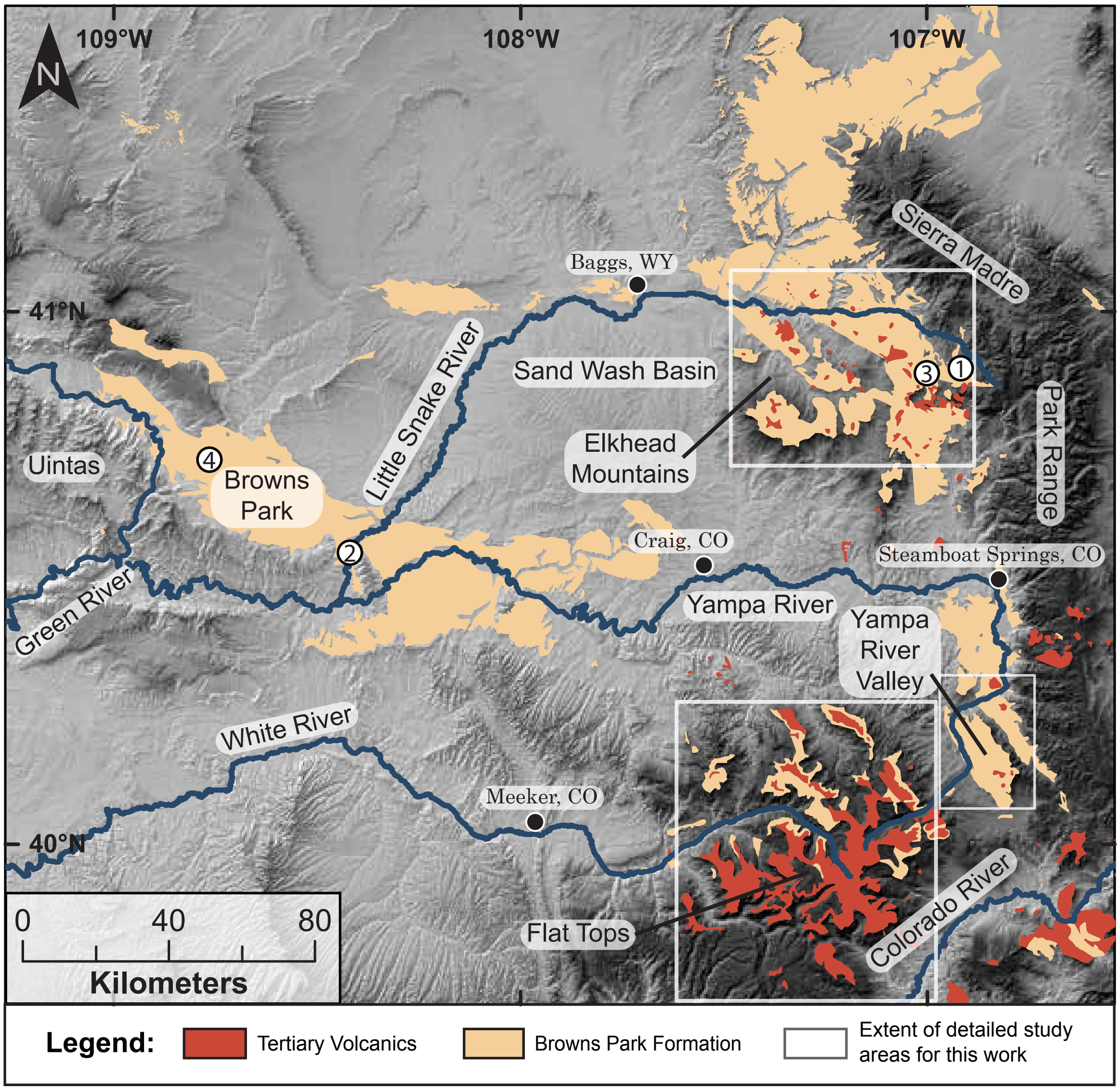


**Rosenberg et al., Figure 4**

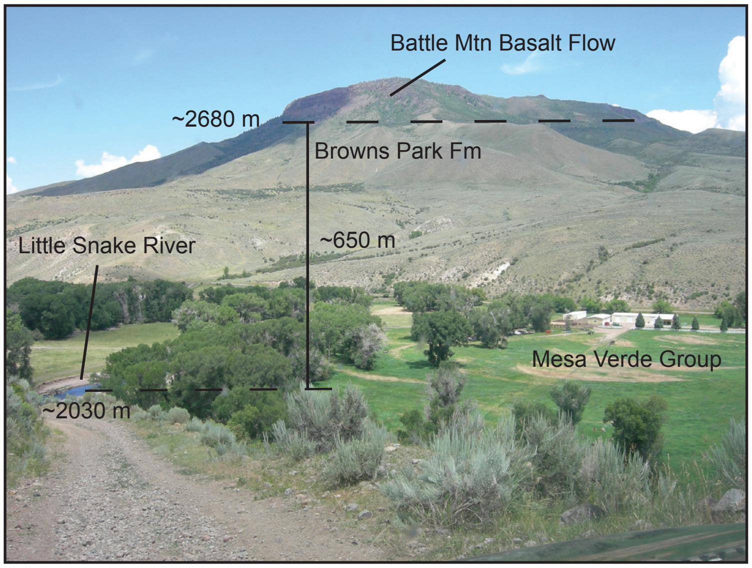


**Rosenberg et al., Figure 5**

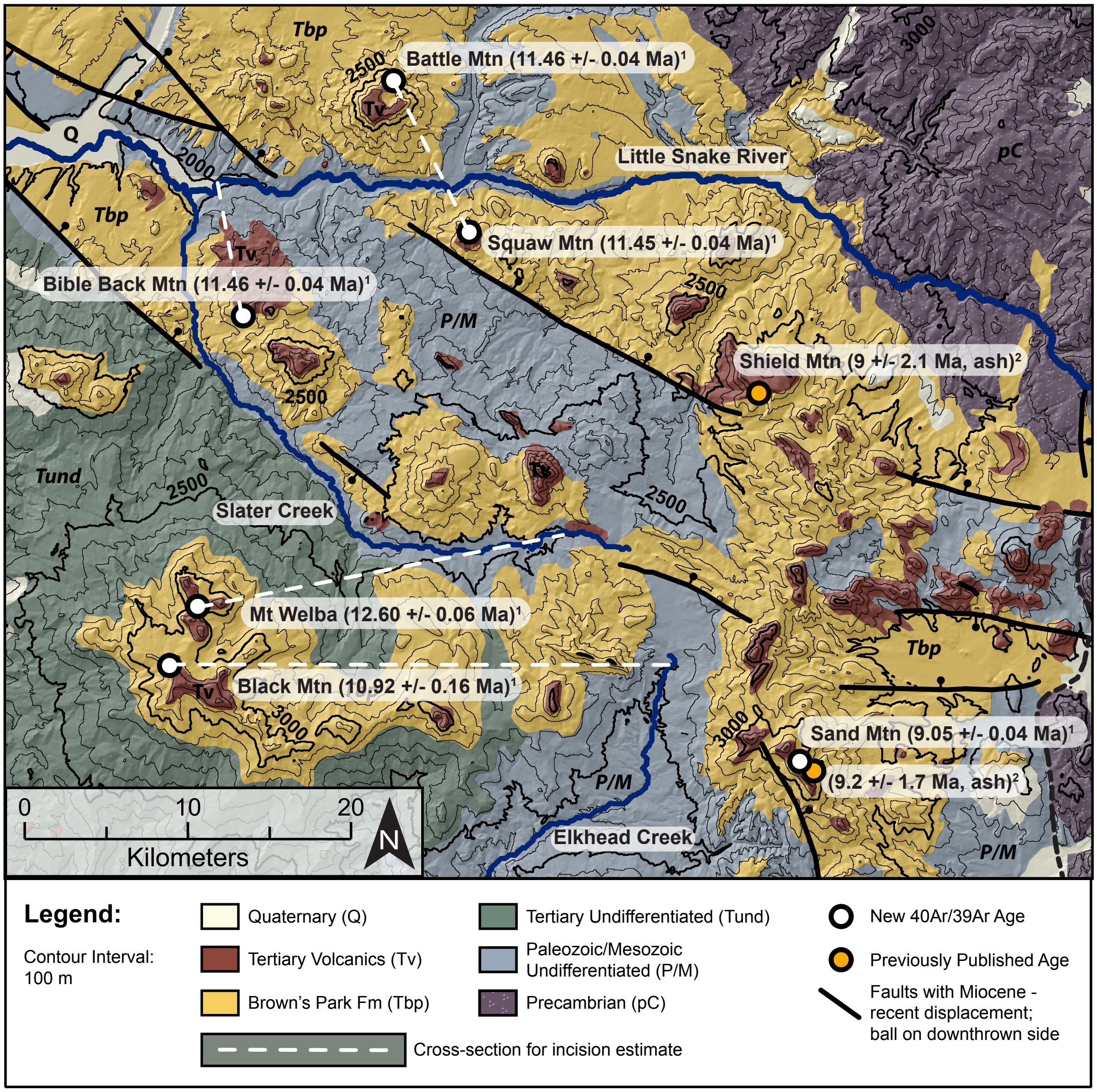


**Rosenberg et al., Figure 6**

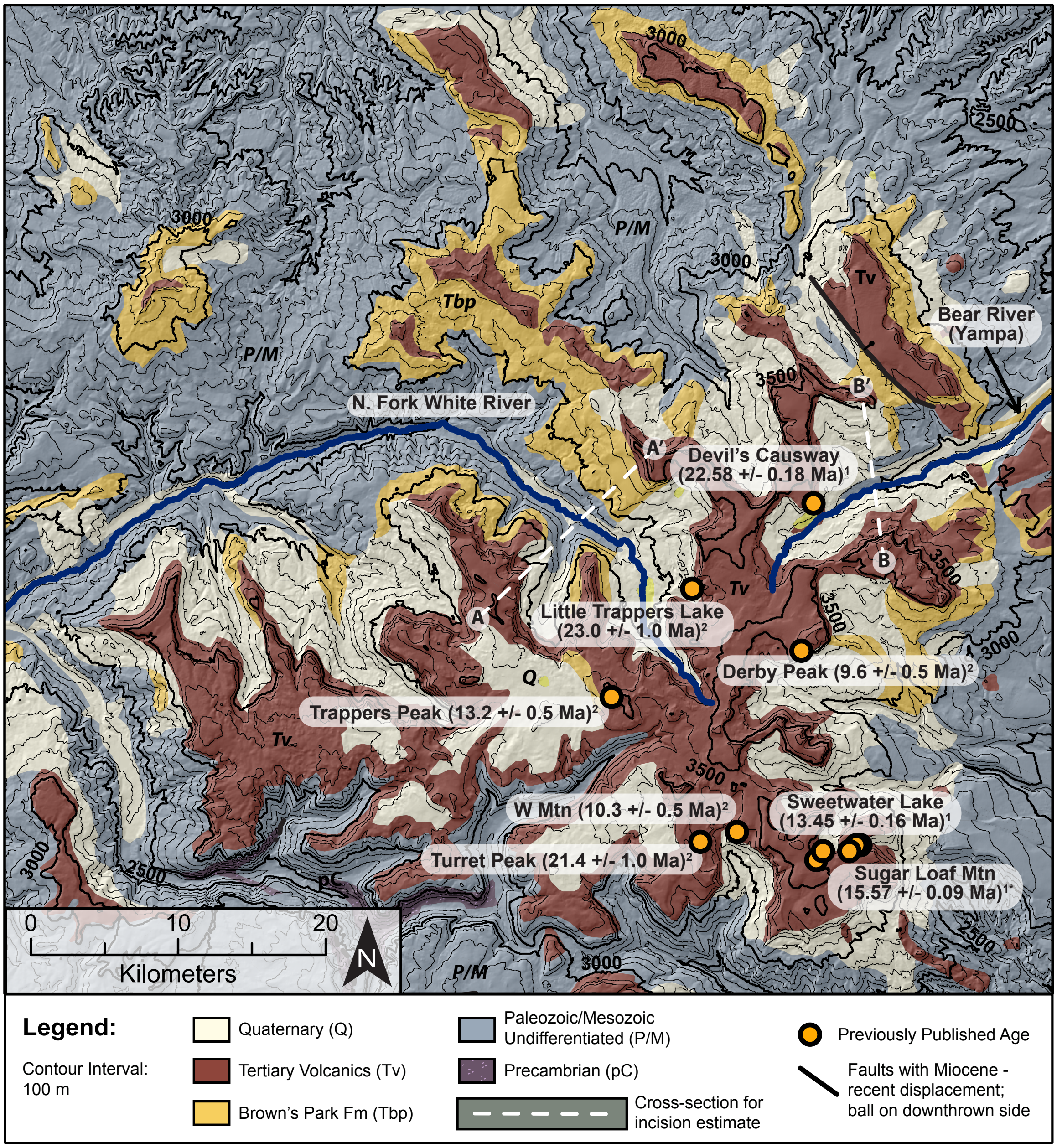


**Rosenberg et al., Figure 7**

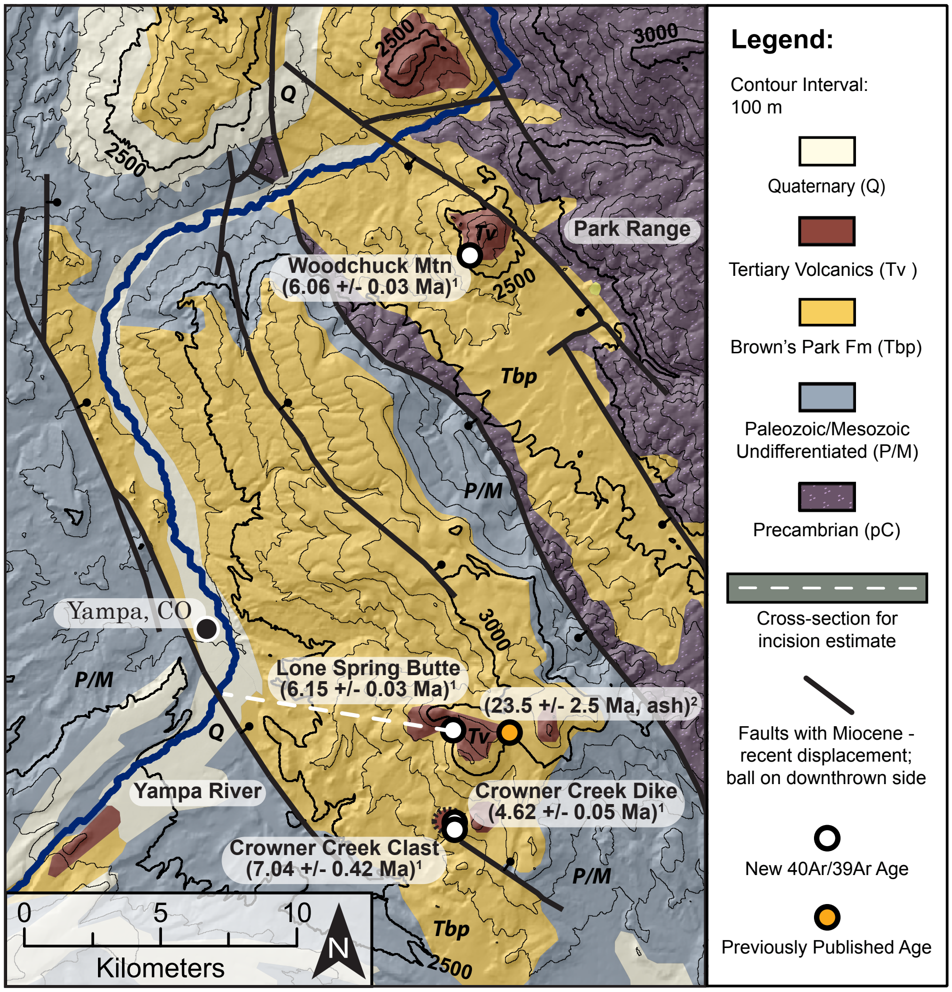


Rosenberg et al., Figure 8

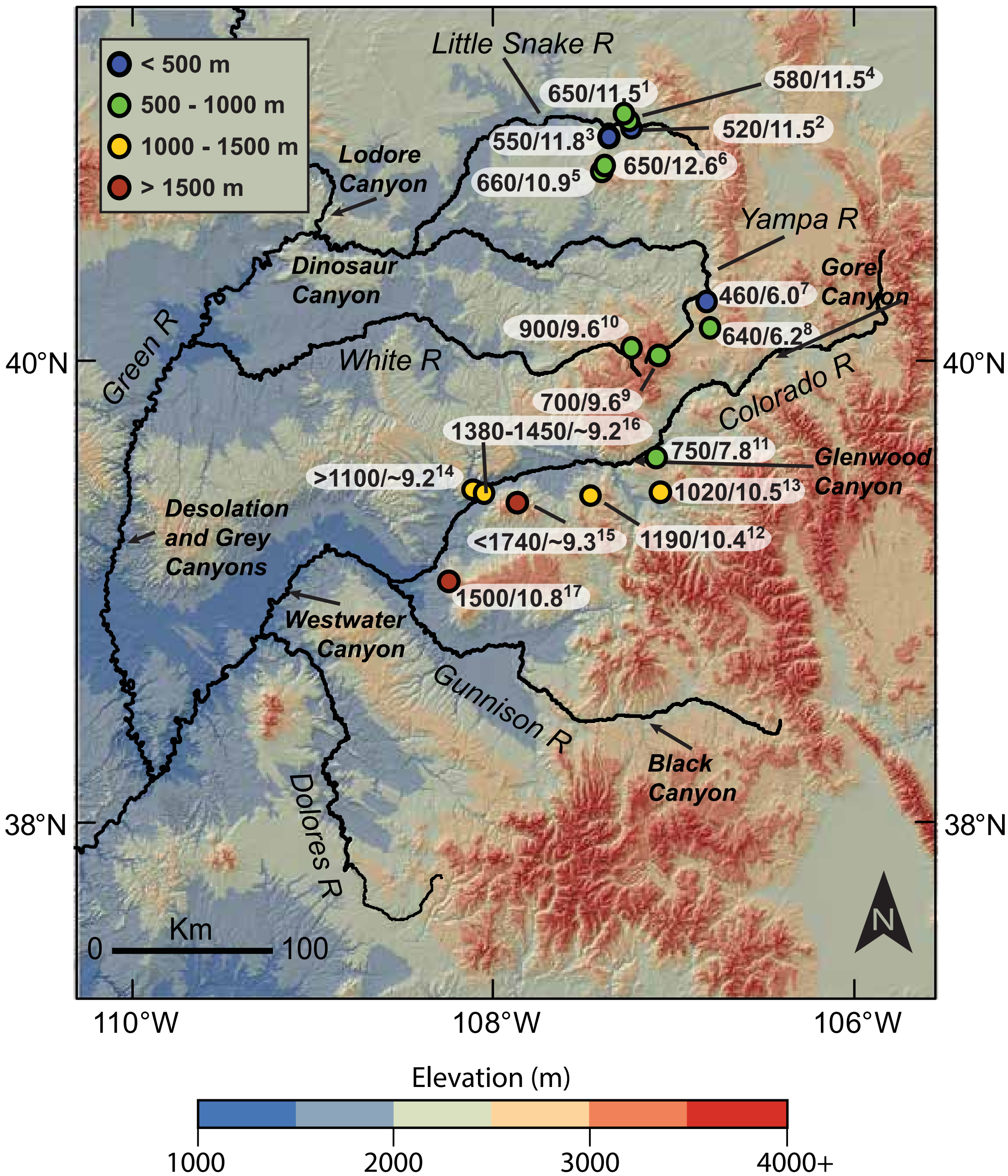


Rosenberg et al., Figure 9

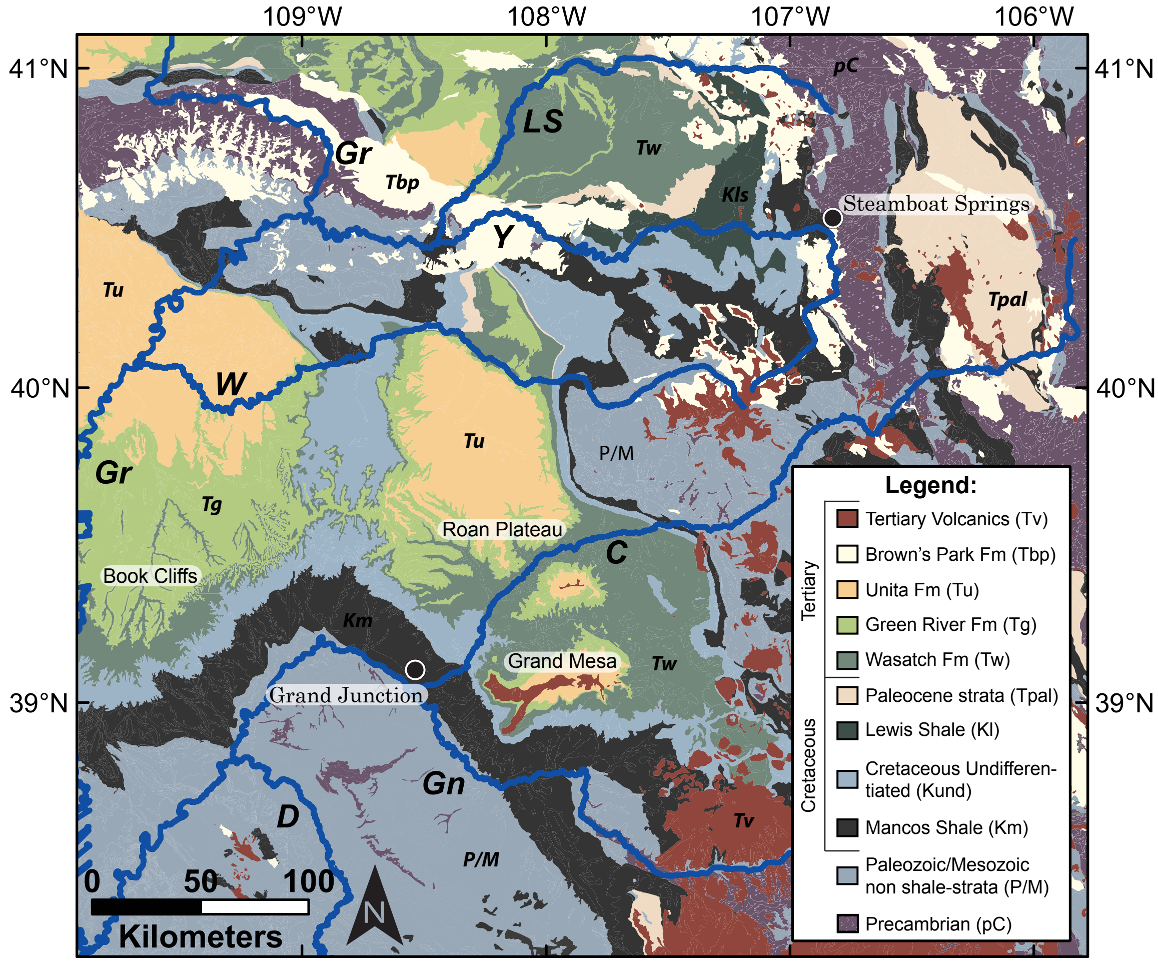


**Rosenberg et al., Figure 10**

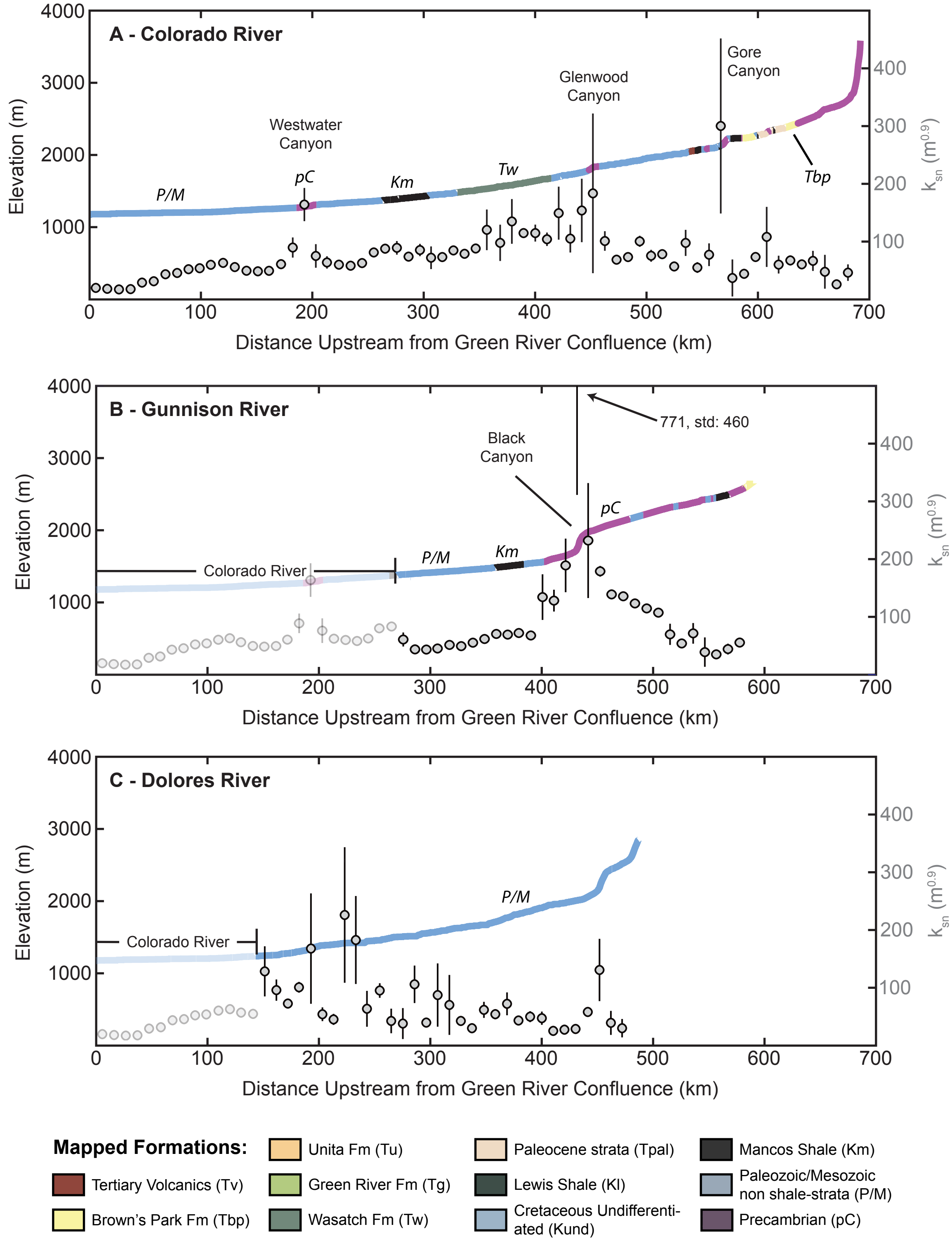


**Rosenberg et al., Figure 11**

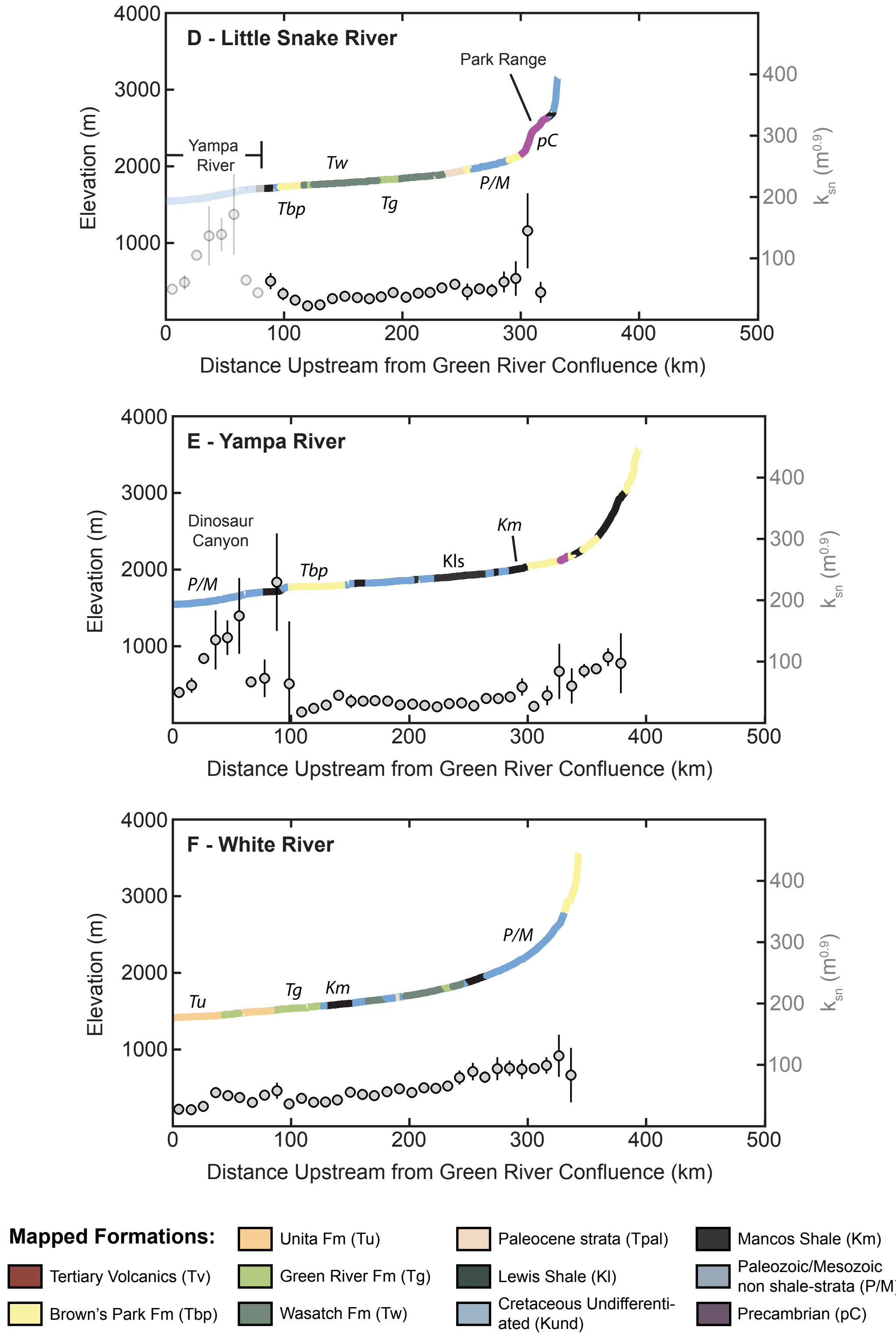


**Rosenberg et al., Figure 11**

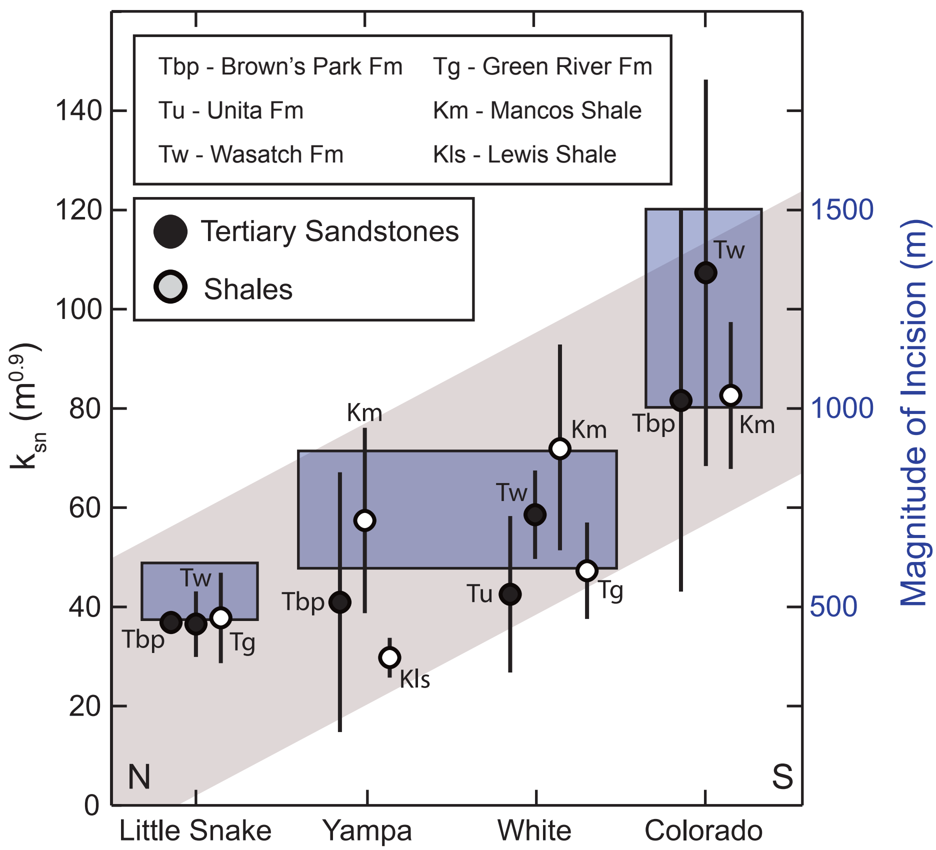


**Rosenberg et al., Figure 12**

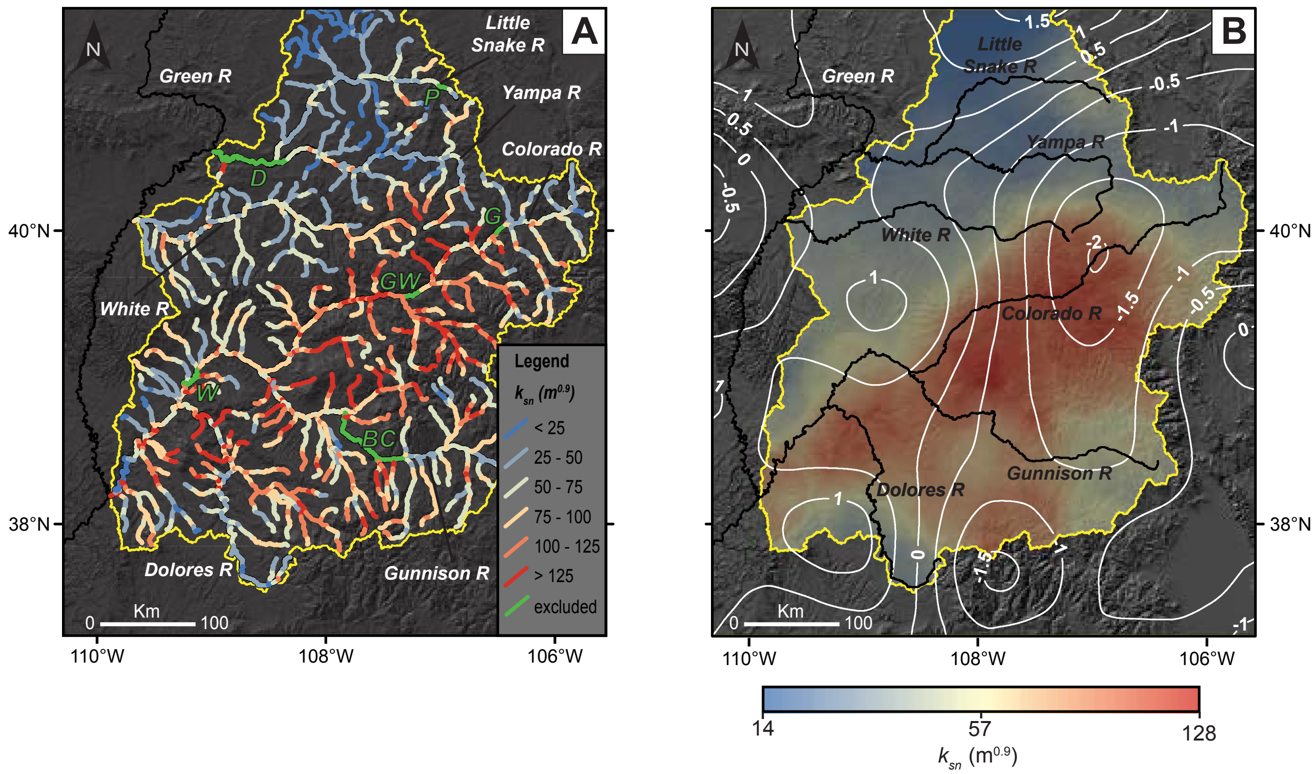


**Rosenberg et al., Figure 13**

TABLE 1. SUMMARY OF CONSTRAINTS ON TIMING AND MAGNITUDE OF INCISION ALONG THE UPPER COLORADO RIVER

| Locality Name | Dating Method | Sample Description | Age (Ma) | Amount of Incision (m) | ~ Time Averaged Incision Rate (m/Ma) | Notes | Figure 8 ID | Data Source |
|---|---|---|---|---|---|---|---|---|
| **Battlement Mesa Area** | | | | | | | | |
| ***Long-term (~10 Ma)*** | | | | | | | | |
| Grand Mesa | $^{40}$Ar/$^{39}$Ar | Basalt flow | 10.76 +/- 0.24 | 1500 | 139 | Basalt flow over Colorado River gravels | 17 | Kunk et al., 2002; Aslan et al., 2010; Cole, 2010 |
| Mount Callahan | $^{40}$Ar/$^{39}$Ar | Basalt boulders | ~ 9.17 | > 1100 | > 120 | Basalt boulders over probable Colorado River gravels | 14 | Berlin et al., 2008, 2009 |
| Battlement Mesa | $^{40}$Ar/$^{39}$Ar | Basalt flows | ~ 9.3 | < 1740 | < 187 | Basalt flow | 15 | Berlin et al., 2008, 2009 |
| Roan Plateau--Battlement Mesa | $^{40}$Ar/$^{39}$Ar | Basalt flow and boulders | ~ 9.3 - 9.17 | 1380-1450 | ~ 148 - 158 | Debris flow slope reconstruction | 16 | Berlin et al., 2008; Berlin, 2009; this study |
| Little Baldy Mountain | $^{40}$Ar/$^{39}$Ar | Basalt flow | 10.38 +/- 0.12 | 1190 | 115 | Basalt flow over fluvial gravels of uncertain provenance | 12 | Kunk et al., 2002; Aslan, pers comm |
| ***Short-term (~0.5-2 Ma)*** | | | | | | | | |
| Grass Mesa | $^{26}$Al/$^{10}$Be burial age | Shielded quartz clast | 1.77 +0.71/-0.51 | 225 | 127 | Elevation of strath terrace above river | n/a | Berlin et al., 2008, 2009 |
| Morrisana Mesa | $^{26}$Al/$^{10}$Be burial age | Drill cuttings | 0.44 +/- 0.3 | 94 | 214 | Elevation of strath terrace above river | n/a | Darling et al., 2012 |
| **Glenwood Canyon Area** | | | | | | | | |
| ***Long-term (~10 Ma)*** | | | | | | | | |
| Basalt Mountain | $^{40}$Ar/$^{39}$Ar | Basalt flow | 10.49 +/- 0.07 | 1020 | 97 | Basalt flow associated with fluvial gravels of uncertain provenance | 13 | Kunk et al., 2002; Aslan et al., 2010 |
| Spruce Ridge | $^{40}$Ar/$^{39}$Ar | Basalt flow | 7.8 +/- 0.04 | 750 | 96 | Basalt flow over probable Colorado River gravels | 11 | Kunk et al., 2002; Kirkham et al., 2001; Brown et al., 2007 |
| ***Short-term (~0.5-2 Ma)*** | | | | | | | | |
| Gobbler Knob | $^{40}$Ar/$^{39}$Ar | Basalt flow | 3.03 +/- 0.02 | 732 | < 242 | Basalt flow directly on bedrock | n/a | Kunk et al., 2002 |
| Dotsero | $^{40}$Ar/$^{39}$Ar | Lava Ck B tephra | 0.639 +/- 0.002 | 85 | 133 | Lava Ck B tephra ~10 m above Colorado River gravels | n/a | Dethier, 2001; Lanphere et al., 2002 Aslan et al., 2010 |

TABLE 2.  SUMMARY OF NEW CONSTRAINTS ON INCISION ALONG TRIBUTARIES OF THE UPPER GREEN RIVER

| Locality Name | Dating Method | Sample Description | Measured Age (Ma) | Amount of Incision (m) | ~ Time Averaged Incision Rate (m/Ma) | Local Thickness of Browns Park Formation (m) | Notes | Figure 8 ID |
|---|---|---|---|---|---|---|---|---|
| **Little Snake River** | | | | | | | | |
| Battle Mountain | $^{40}Ar/^{39}Ar$ | Basalt flow | 11.46 +/- 0.04 | 650 | 57 | 620 | Relief to Little Snake River | 1 |
| Squaw Mountain | $^{40}Ar/^{39}Ar$ | Basalt flow | 11.45 +/- 0.04 | 520 | 45 | 510 | Relief to Little Snake River | 2 |
| Bible Back Mountain | $^{40}Ar/^{39}Ar$ | Basalt flow | 11.81 +/- 0.04 | 550 | 47 | 450 | Relief to Little Snake River | 3 |
| Battle/Squaw (average) | $^{40}Ar/^{39}Ar$ | Basalt flows | ~ 11.45 +/- 0.04 | 580 | 51 | ~ 480 | Land surface reconstruction (x-sec) | 4 |
| Black Mountain | $^{40}Ar/^{39}Ar$ | Mafic-intermediate flow | 10.92 +/- 0.16 | 660 | 60 | 350 | Relief to tributary (Elkhead Creek) | 5 |
| Mt Welba | $^{40}Ar/^{39}Ar$ | Basalt flow | 12.60 +/- 0.06 | 650 | 52 | 400 | Relief to tributary (Slater Creek) | 6 |
| **Yampa River** | | | | | | | | |
| Woodchuck Mountain | $^{40}Ar/^{39}Ar$ | Basalt flow | 5.97 +/- 0.06 | 460 | 77 | 460 | Relief to Yampa River | 7 |
| Lone Spring Butte | $^{40}Ar/^{39}Ar$ | Basalt flow | 6.15 +/- 0.03 | 630 | 102 | 630 | Relief to Yamap River | 8 |
| Orno Pk--Flat Top Mtn | $^{40}K/^{39}Ar$ | Basalt flows | ~9.6 +/- 0.5 | 700 | 73 | ~ 200 | Land surface reconstruction (x-sec); dates from Larsen et al., 1975 | 9 |
| **White River** | | | | | | | | |
| Lost Lakes Pk--Sable Pt | $^{40}K/^{39}Ar$ | Basalt flows | ~9.6 +/- 0.5 | 900 | 94 | ~ 300 | Land surface reconstruction (x-sec); dates from Larsen et al., 1975 | 10 |

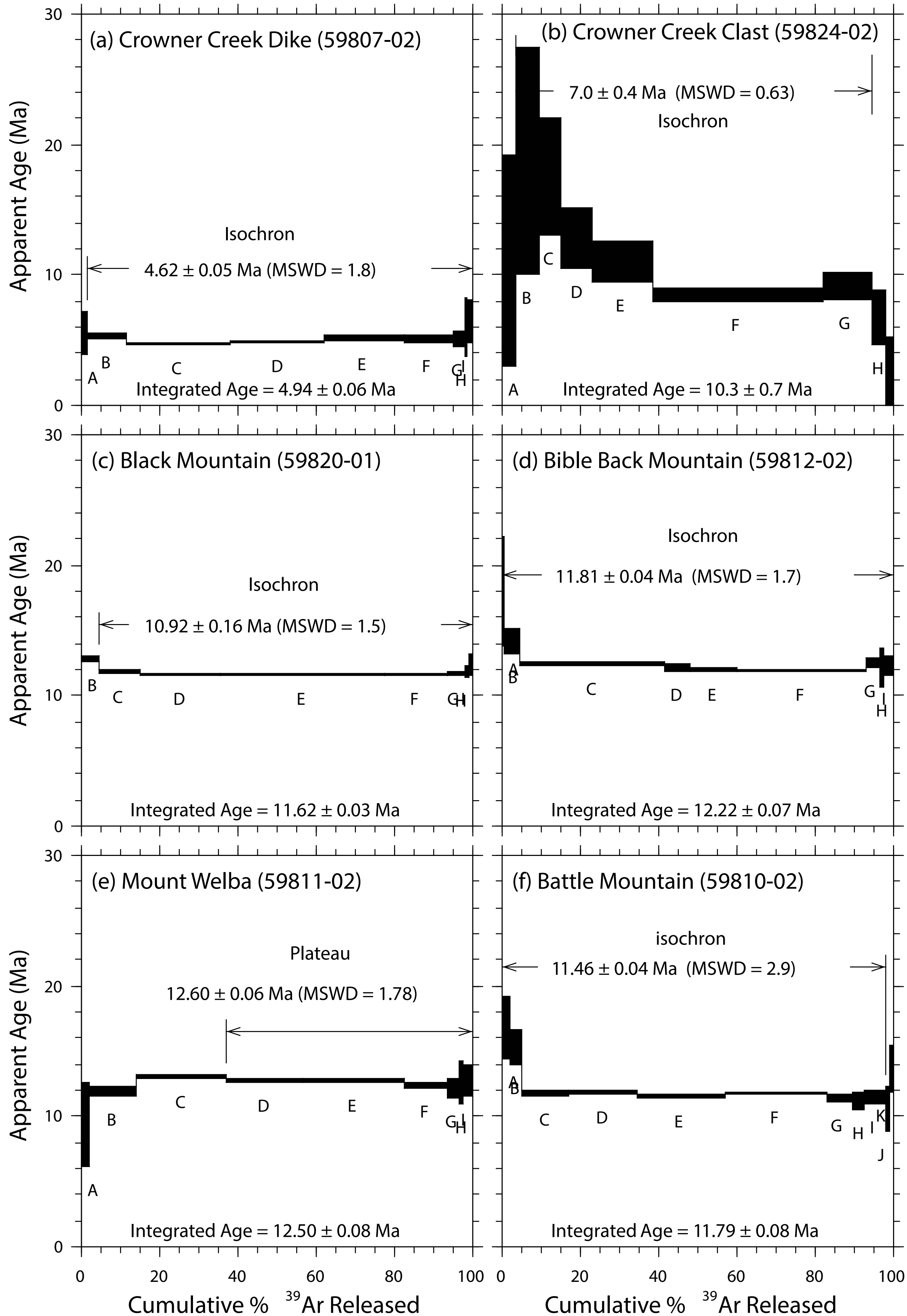


**Figure A-1:** Age spectra diagrams.

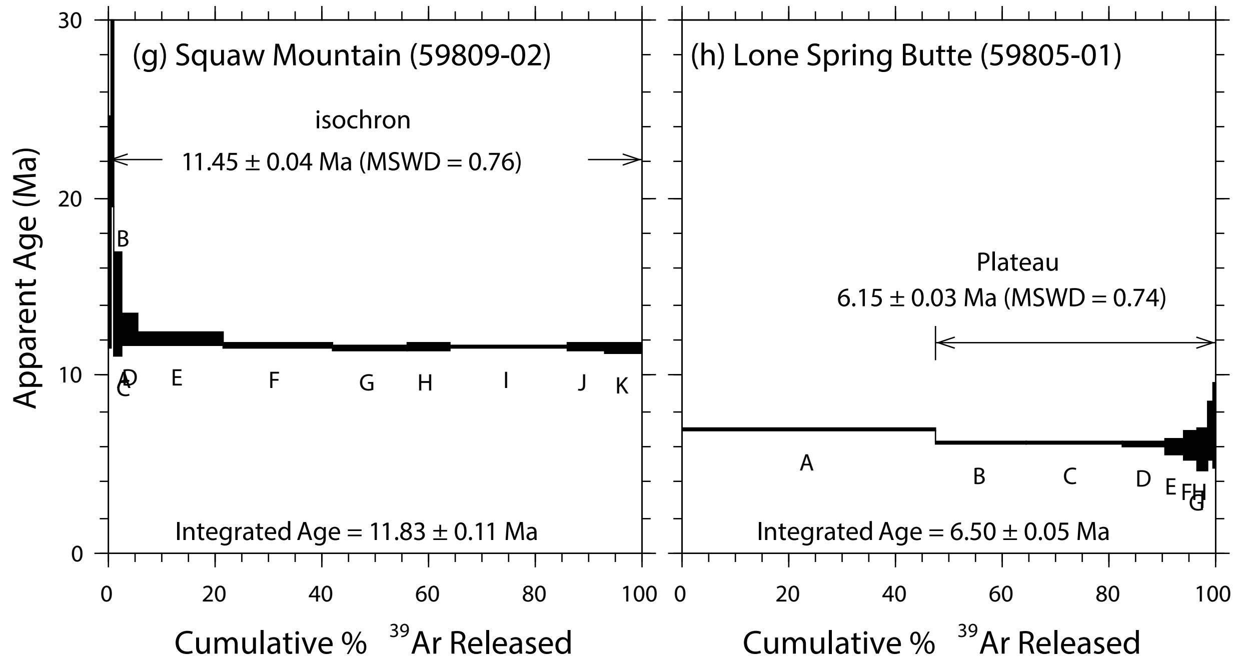


**Figure A-1:** Age spectra diagrams.

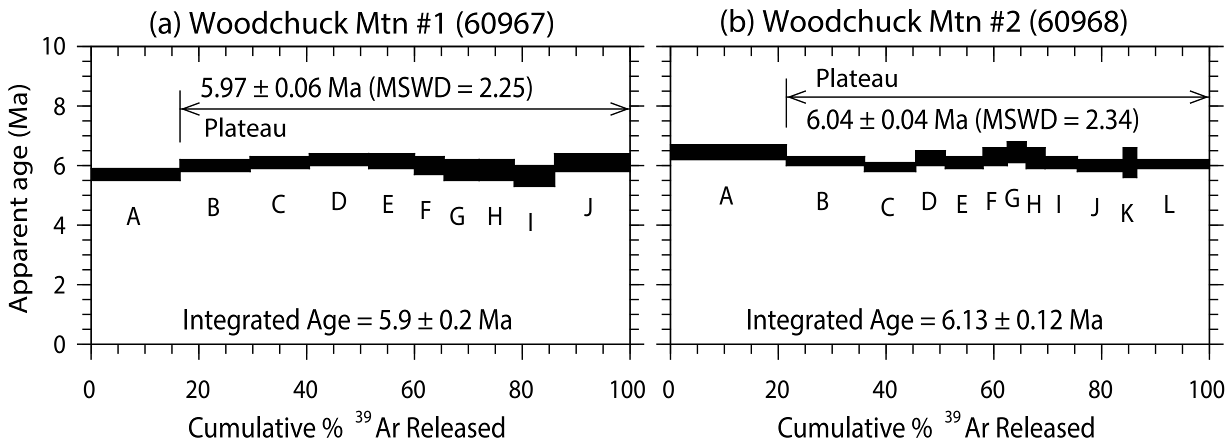


**Figure A-2:** Age spectra diagrams.

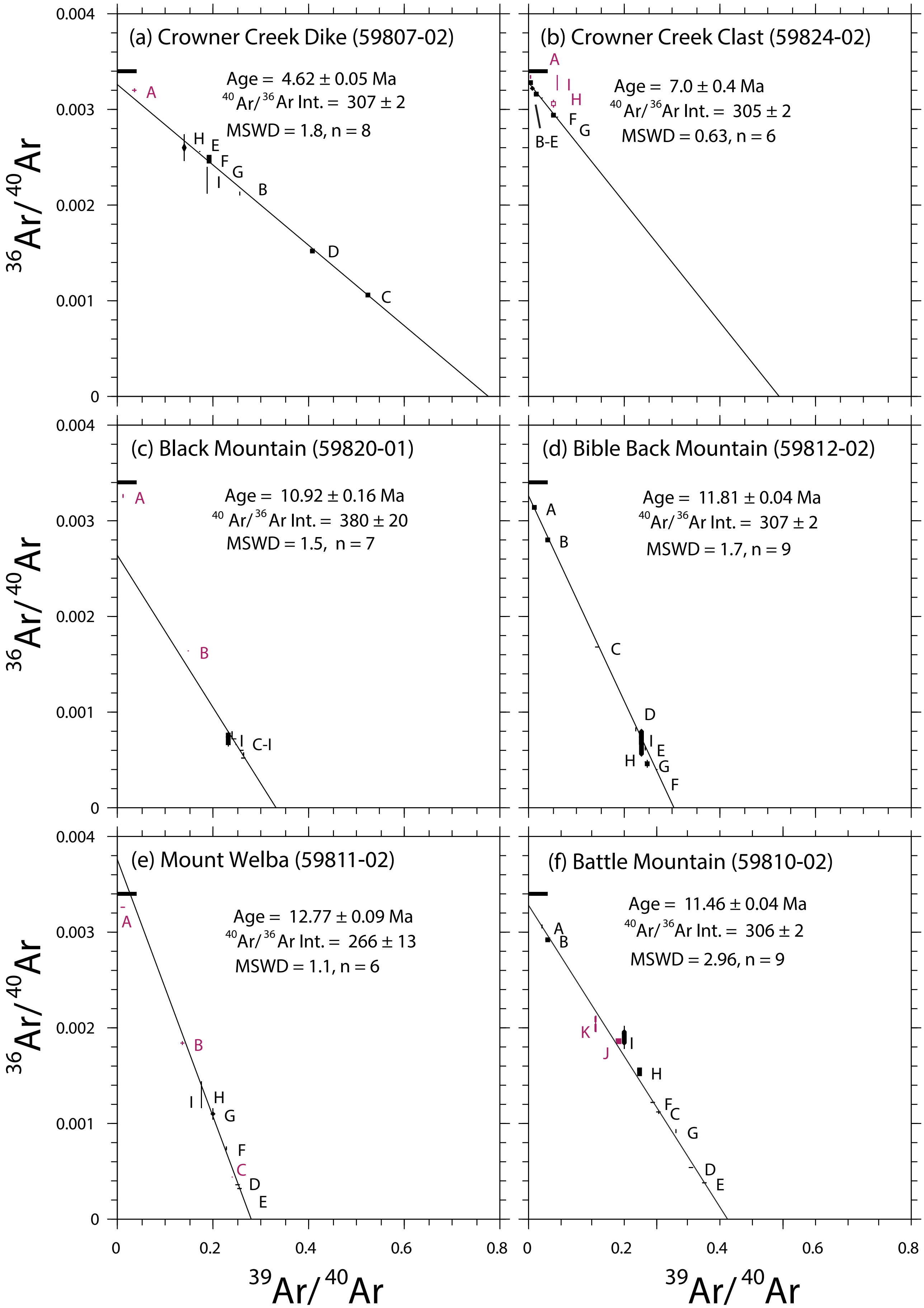


**Figure A-3:** Isochron diagrams. Data shown in black are used for regressions.

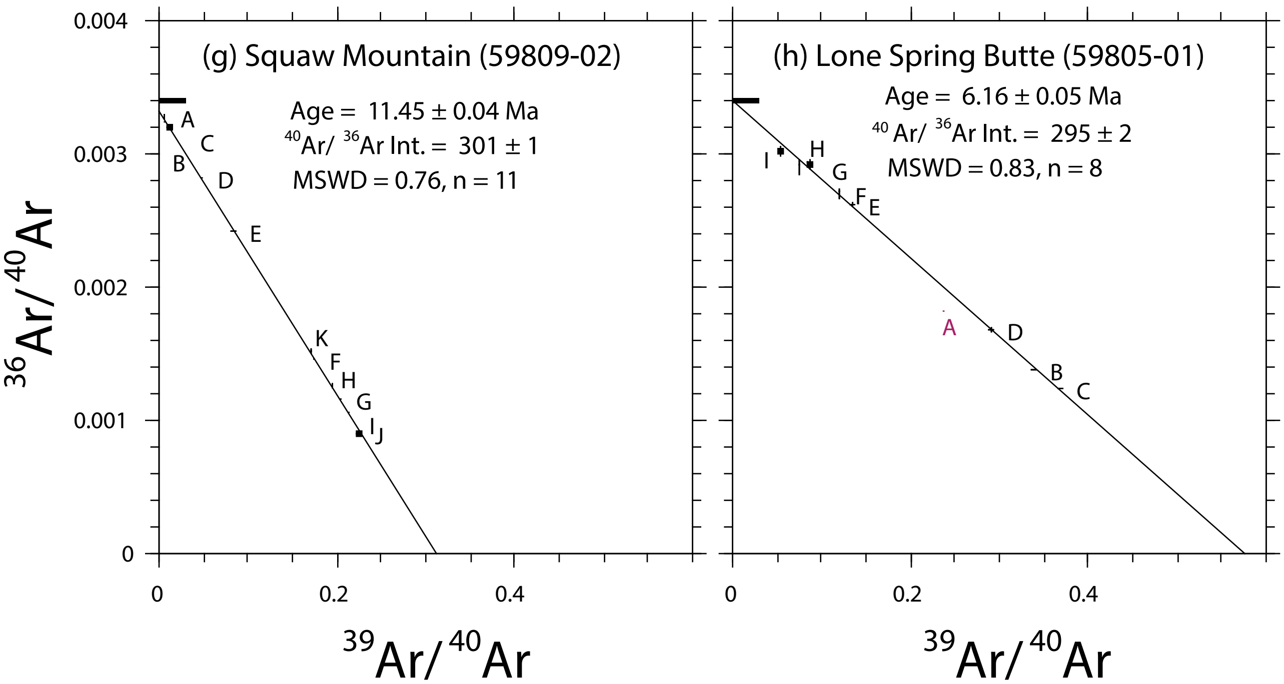


**Figure A-3:** Isochron diagrams. Data shown in black are used for regressions.

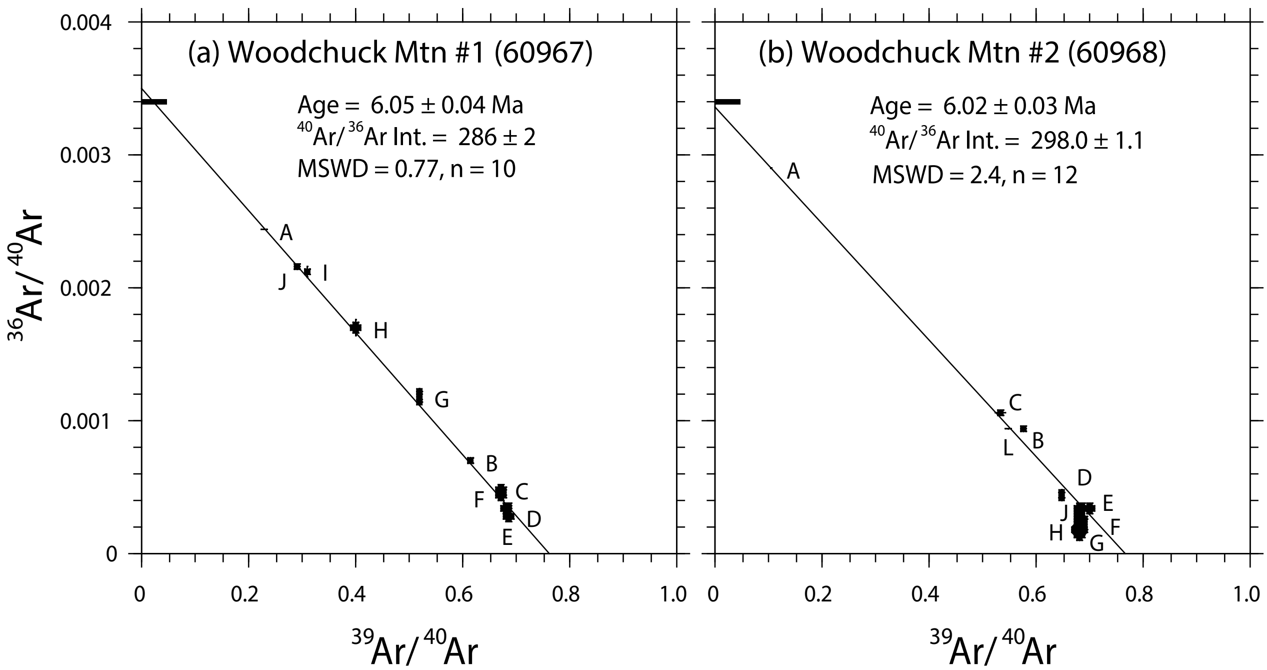


**Figure A-4:** Isochron diagrams. Data shown in black are used for regressions.

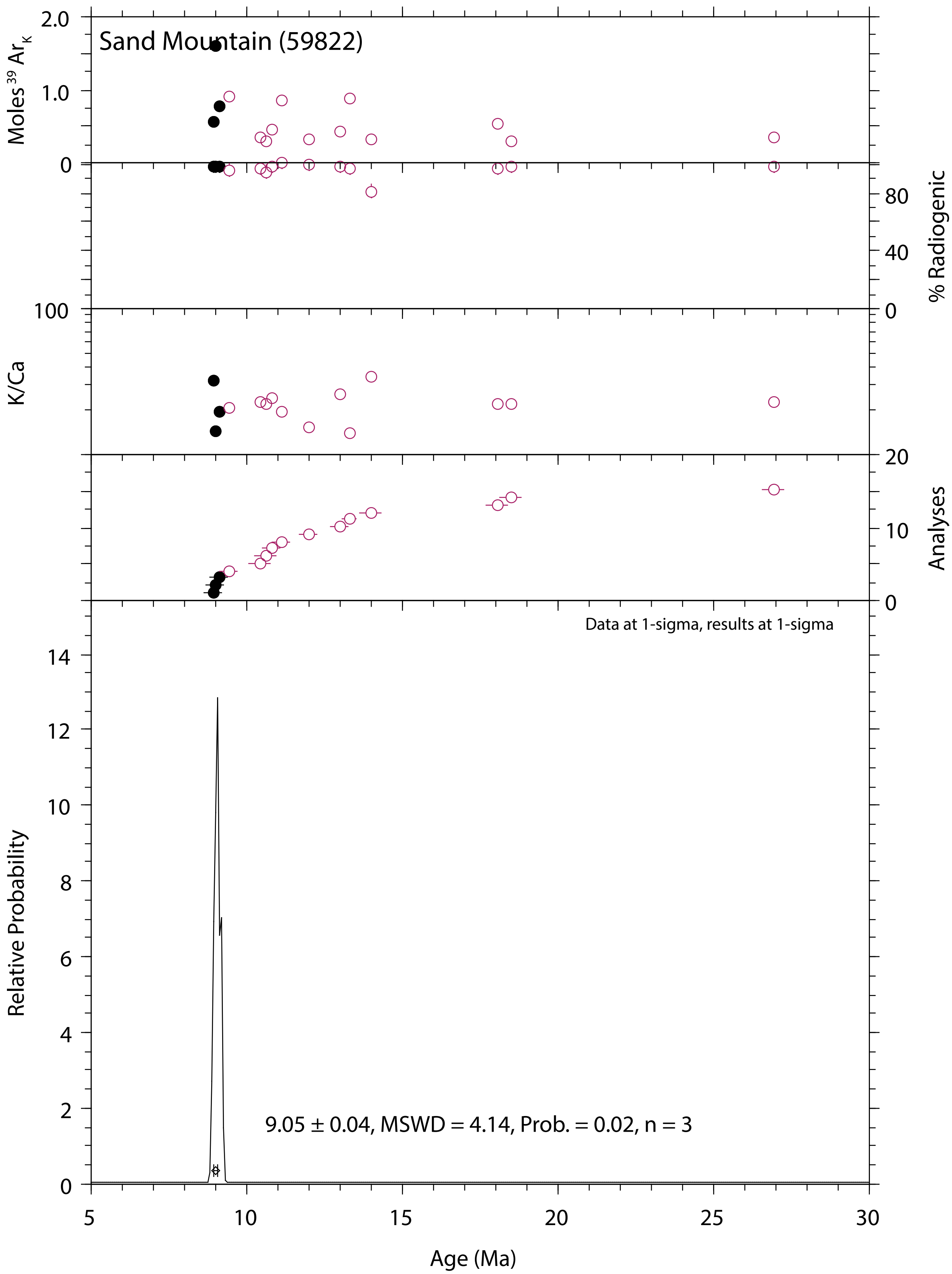


**Figure A-5:** Age probability distribution diagram (sanidine grains)